University of Zurich[UZH]

Wax turnover in sun-exposed and shaded beech leaves (Fagus sylvatica)

GEO 511 Master's Thesis

Author
Tatjana Carina Speckert
10-737-500

Supervised by
PD Dr. Guido Lars Bruno Wiesenberg
Fanny Petibon

Faculty representative
PD Dr. Guido Lars Bruno Wiesenberg

30.09.2019
Department of Geography, University of Zurich

University of Zurich[UZH]

Department of Geography

Wax turnover in sun-exposed and shaded beech leaves (*Fagus sylvatica*)

Master Thesis – GEO 511

September 30^{th}, 2019

Tatjana Carina Speckert

10–737–500

Supervision by: PD Dr. Guido Wiesenberg

Co-supervision by: PhD candidate Fanny Petibon

Member of Faculty: PD Dr. Guido Wiesenberg

Abstract

Plant waxes are of special interest in plant protection as they form a continuous protective layer between a plant and its environment. Particularly, waxes located at the outermost surface, known as epicuticular waxes, play a crucial role in plant protection against moisture loss, UV-radiation as well as fungal and bacterial attacks. However, little is known about how fast epicuticular waxes are renewed, especially in mature plants. Moreover, to what extend epicuticular waxes are renewed through sunlight exposure is not yet fully understood. Hence, to investigate the influence of sun exposure on epicuticular wax composition and renewal, a $^{13}CO_2$ pulse-chase labelling experiment was conducted in the late growing season (August 2018) on a 200-year-old beech tree (*Fagus sylvatica*) which is located on the Irchel Campus, Zurich, Switzerland. To investigate the epicuticular wax composition and modification throughout the late growing season, sun-exposed and shaded leaves were collected weekly until October 2018 and analysed for *n*-alkane composition whereby the total lipid extract (TLE) as well as *n*-alkane molecular ratios such as average chain length (ACL) and carbon preference index (CPI) were identified. In addition, the compound specific isotope composition ($\delta^{13}C$) of *n*-alkanes was used to identify the time needed for the formation of new waxes.

Sun-exposed leaves showed a larger epicuticular wax content per leaf unit area (+45%) with a larger proportion of *n*-alkanes (+60%) than shaded leaves. *n*-Alkanes of all investigated leaf samples showed a strong odd-over-even predominance with C_{27} as the dominant chain length. The overall ^{13}C-enrichment indicates a significant assimilation of ^{13}C after the labelling experiment with 20-30% in bulk tissue and 1% in *n*-alkanes. Furthermore, the quantity of renewed waxes is equivalent to 0.03 $\mu g\ cm^{-2}$ per day in shaded and 0.8 $\mu g\ cm^{-2}$ per day in sun-exposed leaves, indicating a significant faster wax renewal rate in sun-exposed leaves compared to shaded leaves. This faster wax renewal rate is mainly regulated by the external environment, particularly light exposure. This study sheds light on the relationship between leaf wax formation in relation to environmental stress, including sun exposure. This contributes to a better understanding of a plant's metabolism and growth in response to high sunlight and temperature environments, which will become increasingly important in the upcoming century.

Declaration

I hereby declare that the submitted thesis is the result of my own independent work. All external sources are explicitly acknowledged in this thesis.

Klingnau, September 30^{th} 2019

Speckert, Tatjana Carina

Acknowledgements

First of all I would like to thank my supervisors PhD candidate Fanny Petibon and PD Dr. Guido Wiesenberg for their willingness to support this master thesis. The door to their offices was always open whenever I had a question. I am thankful for their confidence, their great support during the laboratory work and the helpful inputs and advices. I also want to thank the Soil and Biogeochemistry group of the Department of Geography with a special thank to Tatjana Kraut, Cyrill Zosso and Nicholas O.E. Ofiti for their support.

I also want to thank my family and friends for their support and sympathy.

Abbreviations

ACL	Average Chain Length
$\delta^{13}C$	Stable carbon isotope
CPI	Carbon Preference Index
DCM	Dichloromethane (CH_2Cl_2)
DW	Dry Weight
Fraction A	Aliphatic Hydrocarbons
Fraction B	Aromatic Hydrocarbons
Fraction C	Low polar Heterocompounds
Fraction N	Neutral Lipids
Fraction H	Free Fatty Acids
Fraction P	Polar and High Molecular Weight Compounds
FW	Fresh Weight
GC-C-irMS	Gas Chromatography Carbon Isotope Mass Spectrometry
GC-FID	Gas Chromatography-Flame Ionization Detector
GC-MS	Gas Chromatography-Mass Spectrometry
KOH	Potassium Hydroxide
MeOH	Methanol (CH_3OH)
SPAD	Soil Plant Analysis Development
SPE	Solid Phase Extraction
TC	Total Carbon
TLE	Total Lipid Extract
TN	Total Nitrogen
UV	Ultra Violet
VPDB	Vienna Pee Dee Belemnite

Contents

List of Figures

List of Tables

1 Introduction

Plant waxes are a natural key innovation which play an important role in the survival and development of terrestrial plants (Koch *et al.*, 2009). Through evolution, terrestrial plants developed a protective outermost wax layer, known as plant cuticle. The plant cuticle is composed of cutin and hydrophobic components (Reina-Pinto and Yephremov, 2009) and mainly protects the plant against deleterious water loss (Buschhaus *et al.*, 2007). Other functions, like the protection against damage from UV-radiation, droughts as well as against fungal and insect attacks have also been investigated (Eglinton and Hamilton, 1967; Hauke and Schreiber, 1998; Dodd and Poveda, 2003; Kunst and Samuels, 2003; Feakins *et al.*, 2016; Ardenghi *et al.*, 2017; Laila *et al.*, 2017; Nelson *et al.*, 2017). Particularly, epicuticular wax that is located at the outermost plant surface is of special interest in plant protection as one of the most protective barriers against harmful environmental impacts (Nguyen-Tu *et al.*, 2001; Samuels *et al.*, 2008; Bernhard and Joubès, 2013). Typical epicuticular wax components are *n*-alkyl lipids including *n*-alcohols, *n*-alkanes, *n*-alkanoic acids and *n*-esters (Eglinton and Eglinton, 2008; Jetter and Kunst, 2008; van Maarseveen and Jetter, 2009) whereby *n*-alkanes are among the most abundant occurring component of leaf waxes (Ardenghi *et al.*, 2017). Various authors e.g. Kolattukudy and Walton (1973), Jetter *et al.*(2000), Kunst and Samuels (2003), Müller and Riederer (2005), Bargel *et al.* (2006), Jetter and Kunst (2008), Koch *et al.* (2009), give a wide array of overviews on biosynthesis, function and chemical composition of epicuticular waxes.

An increased epicuticular wax content can be found in plants exposed to intense solar radiation which is associated with low water availability (Shepherd and Griffiths, 2006) as observed in numerous plants like beech trees (*Fagus sylvatica*; Prasad and Gülz, 1990), walnut trees (*Juglans regia* L.; Lacointe *et al.*, 2004) as well as in wheat grass (Jefferson *et al.*, 1989). Moreover, epicuticular wax content is highly dynamic throughout one growing season (Chikaraishi *et al.*, 2004) as it is regularly removed by wind or dust abrasion (Conte *et al.*, 2003), insects (Feakins *et al.*, 2016) and leaf to leaf contact (Knight *et al.*, 2004). Hence, changes in epicuticular wax content and composition are considered as an adaptation to local environments (Klich, 2000; Bernhard and Joubès, 2013). In addition, variability in epicuticular wax content and its composition are also caused by ontogeny (Diefendorf *et al.* 2011), plant species and plant growth (Bush and McInerney, 2013). For instance, Bush and McInerney (2013) observed variations in the epicuticular wax composition, specifically in the *n*-alkane content, between leaves of shaded and sun-exposed canopy positions within the same tree. These differences are mainly due to micro-climatic factors like sun exposure (van Wittenberghe *et al.*, 2012), wind ablation as well as washing off by intense rainfall (Gao *et al.*, 2012). Therefore, it is also suggested that the renewal rate of epicuticular waxes might depend on environmental conditions (e.g. sunlight exposure) and thus varies at different canopy positions within the same tree (Bush and McInerney, 2013). Leaf properties like the leaf area and leaf lifespan are also considered to influence epicuticular wax content and its renewal (Mueller *et al.*, 2012). However, the rate of wax renewal due to environmental stress is unknown, particularly in relation to sun exposure. Moreover,

many studies focus on summer leaves of rather young trees (Jetter and Schäffer, 2001; Dyckmans *et al.*, 2002; Nogués *et al.*, 2006). As a consequence, there is a lack of knowledge about how fast the epicuticular wax is renewed in leaves of mature plants in the late growing season, specially in high sunlight conditions.

Long chain *n*-alkanes (C_{27} to C_{33}) with a typically strong odd-over-even predominance are valuable molecular proxies as plant derived lipids are released into the environment as leaf fragments or as aerosols (Eglinton and Eglinton, 2008) and transported over substantial distances until they are deposited in soils or lake sediments (Jansen and Wiesenberg, 2017). They have further been used to reconstruct continental vegetation patterns, including climate induced changes (Eglinton and Eglinton, 2008; Vogts *et al.*, 2009), as well as to identify present-day carbon allocation in plant-soil systems (Li *et al.*, 2018). The utility of long chain *n*-alkanes as a reliable molecular proxy is further strengthened by their chemical inertness and environmental persistence (Eglinton and Eglinton, 2008; Wiesenberg *et al.*, 2009) as well as by an easy extraction and analysis (Diefendorf and Freimuth, 2017). Moreover, by using long-chain *n*-alkanes as molecular proxies the distribution is typically related to the average chain length (ACL), carbon preference index (CPI) and stable isotope concentration (Eglinton and Eglinton, 2008) since *n*-alkane distribution is sensitive to environmental changes (Hoffmann *et al.*, 2013). Nevertheless, it still remains unclear which factors control the renewal rate of epicuticular wax and whether these can be traced by such molecular ratios. Thus, studies examining the renewal rate of epicuticular wax are missing.

Aside from the variability in *n*-alkane content, compound specific $\delta^{13}C$ analysis has also been used to investigate the effects of environmental factors such as sun exposure, increased temperatures and droughts (Lockheart *et al.*, 1997; Nguyen-Tu *et al.*, 2001; Blessing *et al.*, 2015) on changes in plant populations (Wiesenberg *et al.*, 2004). Since plants discriminate $\delta^{13}C$ during photosynthesis, the magnitude of this effect reflects a plant's growth and metabolism in relation to its external environment (Pancost and Boot, 2004). Moreover, fractionation against ^{13}C varies depending on environmental factors like solar radiation (Zimmerman and Ehleringer, 1990), increased temperatures as well as the availability of nitrogen (Dawson *et al.*, 2002). Additionally, leaf properties such as leaf thickness (Vitousek, 1990), leaf ageing (Li *et al.*, 2016) leaf size, stomatal density or canopy position are also suggested to influence fractionation against ^{13}C (Dawson *et al.*, 2002; Bender *et al.*, 2017). To investigate the magnitude of ^{13}C fractionation in lipid biosynthesis, the use of pulse-labelling experiments ($\delta^{13}CO_2$, $\delta^{14}CO_2$) is a common practise (Dawson *et al.*, 2002). It is used to trace carbon allocation and its partitioning among different plant organs (Wiesenberg *et al.*, 2009; Epron *et al.*, 2012). Especially, short pulse-labelling experiments with $^{13}CO_2$ have been implemented for years whereby whole plants or plant parts are exposed to a $^{13}CO_2$-enriched atmosphere in a time frame from several minutes up to several hours (Epron *et al.*, 2012).

Since droughts lead to a ^{13}C-enrichment in plant tissue (Zhang *et al.*, 2019), it is suggested that the exposure to direct sunlight has the same effect and thus tends to increase $\delta^{13}C$ values in sun-exposed leaves. Moreover, it is known that plant lipids of leaf waxes (e.g. *n*-alkanes) in sun-exposed leaves

show a ^{13}C-enrichment due to the coupling of photosynthesis and isotope fractionation in lipid biosynthesis (Collister *et al.*, 1994; Zhang *et al.*, 2019). Nevertheless, there are only a few studies that examine the difference in $\delta^{13}C$ values between bulk tissue and *n*-alkanes in relation to sun exposure, especially with regards to the modification and renewal of epicuticular waxes.

The goals within this study were to identify the variability in the epicuticular wax content, its modification as well as to identify the rate of epicuticular wax renewal in leaves of a mature beech tree (*Fagus sylvatica*), especially in relation to sun exposure throughout the late growing season. Specifically, it was investigated whether an epicuticular wax renewal takes place at all in a mature tree and if so, how fast this wax renewal occurs depending on sun exposure. The questions addressed where:

(1) How does epicuticular wax content differ between sun-exposed and shaded leaves throughout the late growing season?

(2) How fast are epicuticular waxes renewed as a response to sun exposure?

To address these questions, a $\delta^{13}CO_2$ pulse-chase labelling experiment was conducted on a approximately 200-year-old beech tree (*Fagus sylvatica*) in early August 2018 followed by weekly leaf sampling until early October 2018 to examine the composition and rate of renewal of epicuticular waxes in relation to sun exposure. The study followed the hypotheses:

(1) The epicuticular wax content, including *n*-alkane content per leaf unit area, is larger in sun-exposed leaves than in shaded leaves.

(2) The rate of epicuticular wax renewal is faster in sun-exposed than in shaded leaves.

2 Materials and methods

2.1 Study area

Leaves of a mature (200-year-old) beech tree (*Fagus sylvatica*) located on the Irchel Campus, University Zurich, Switzerland [47°23'44" N, 8°32'57" E, 540 masl] (Figure 1), were collected from August to October 2018. The mean annual air temperature is 9.3°C and the mean annual precipitation is 1134mm (MeteoSwiss, http://www.meteoschweiz.admin.ch). The physiography of the study area is characterized as slightly undulating with a plant community consisting of European beech (*Fagus sylvatica*), littleleaf linden (*Tilia cordata*), silver birch (*Betula pendula*), hornbeam (*carpinus betulus*), harewood (*Acer pseudoplantanus*) and understory shrubs.

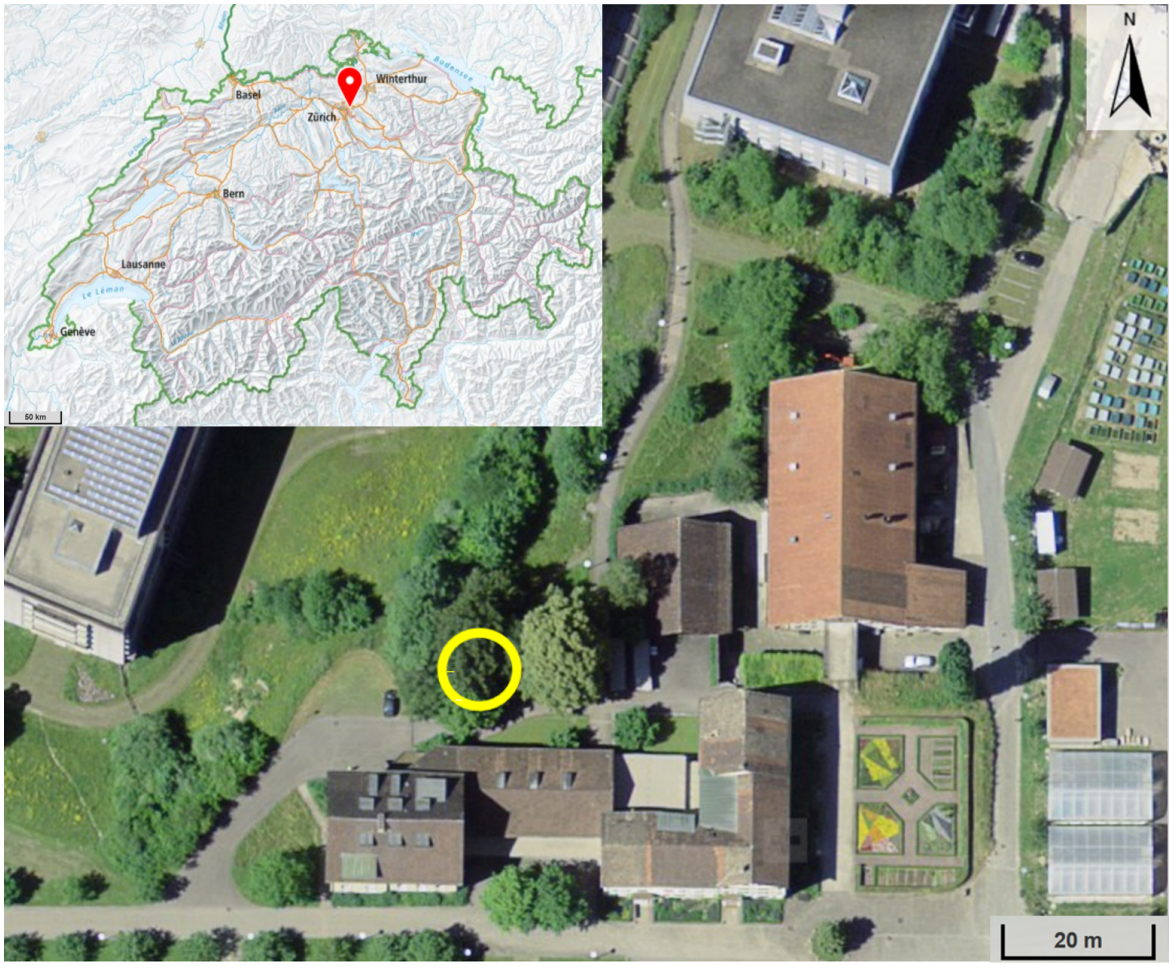

Figure 1: Study area on the Irchel Campus, University Zurich, Switzerland (Swisstopo, http://map.geo.admin.ch).

2.2 $^{13}CO_2$ pulse-chase labelling

The $^{13}CO_2$ pulse-chase labelling experiment was conducted in the late end of the growing season on the 9^{th} of August 2018. Six branches containing approximately 60 leaves each were selected, of which three branches were sun-exposed and three branches were shaded. One additional branch each was used as a control at each site (Supplementary Figures I a and b). For the labelling process, six rectangular shaped labelling chambers (total volume of $0.06m^3$ each) of wire scaffolding were placed underneath the tree and wrapped around the selected branches. Each labelling chamber contained a small glass dish with 1g of sodium hydrogen carbonate ($Na_2\ ^{13}CO_3$) which was completely dissolved in deionized water (Milli-Q quality) (Heinrich *et al.*, 2015). The $^{13}CO_2$ gas was released by injecting 10ml of sulfuric acid (H_2SO_4, 10 atom-%) via syringe directly into the labelling solution. In addition, a small battery driven fan was used to homogeneously distribute the produced $^{13}CO_2$ gas (Srivastava *et al.*, 2017; Kagawa *et al.*, 2005). The air chamber temperature was maintained by ice packs placed between battery driven fan and glass dish (Figures 2a and b). Overall, each branch was exposed to a $^{13}CO_2$-enriched atmosphere for approximately 5 hours at an average air temperature of 38.0°C in the sun and 27.0°C in the shade (Figure 2c).

Potential sources of error during the experiment, which could have negatively affected the $^{13}CO_2$ labelling, were the increased wind velocity that led to a tilted position of the labelling chambers. In addition, the attachment between the plastic covering and the branch had loosened in two chambers due to the increased wind velocity, which resulted in a no longer airtight closure of these chambers and therefore the $^{13}CO_2$ labelling was no longer guaranteed. An additional uncertainty during the experiment was the short running time of the fans as after approximately two hours, the fan stopped running in four of the six chambers, no longer ensuring the homogeneous distribution of the generated $^{13}CO_2$. Furthermore, without the fans the temperature inside the chambers increased (> 30°C) which affects photosynthetic activity as well as the ^{13}C assimilation. As a consequence, only two (n = 1 in sun-exposed and n = 1 in shaded canopy position) of the total six branches, including control, were used to for the lipid analysis and for the identification of the wax renewal rate.

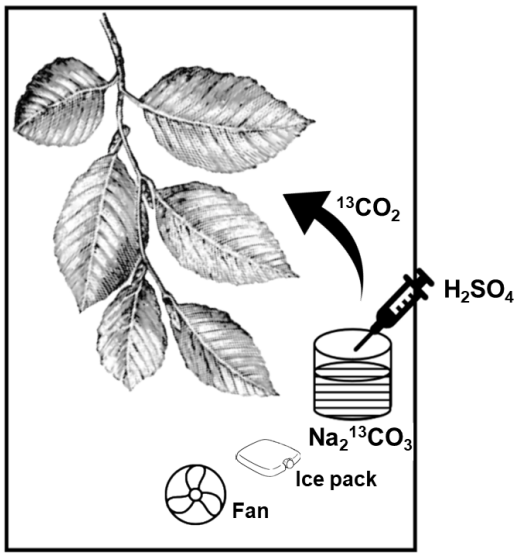

(a) Schematic overview of the labelling chamber. The $^{13}CO_2$ was released by adding 10ml of H_2SO_4 via syringe directly into the labelling solution. The produced $^{13}CO_2$ gas was homogeneously distributed within the labelling chamber by a small battery driven fan (modified after Kawaga *et al.*, 2005).

(b) Labelling chambers were placed on tripods underneath the selected branches.

Figure 2 continues on the next page.

(c) Closed labelling chamber with a selected branch inside.

Figure 2: $^{13}CO_2$ pulse-chase labelling experiment. (Fotos by: Fanny Petibon and Tatjana Speckert, 2018).

2.3 Leaf sampling

The first sampling took place immediately after the labelling chambers were disassembled on the 9^{th} of August, followed by sampling 1, 4 and 7 days later. Afterwards, leaves were sampled weekly until the 11^{th} of October 2018 resulting in a total of 480 leaf samples. Sun-exposed and shaded nodes containing at least three leaves were collected at the topmost and the terminal part of each branch. The three leaves of each node were separated whereby two leaves were used for the analysis of physical leaf properties and one leaf was used for the lipid analysis. After separation, leaves were immediately frozen on dry ice and stored in the laboratory (-80°C) until further analysis.

2.4 Analysis of physical leaf properties

Chlorophyll content was directly measured in the field with a Soil Plant Analysis Development (SPAD) chlorophyll meter. The SPAD meter evaluates the chlorophyll content of the leaf due to the difference in the light attenuation at 650nm (red) and 940nm (infrared), and displays this in SPAD values. Each leaf was placed individually with the adaxial side facing the emitting window of the SPAD chlorophyll meter making sure not to place the emitting window on major veins (Uddling *et al.*, 2007). Five points per leaf were measured of which the average was calculated.

Leaf thickness was measured on fresh leaves left and right of the midrib using a vernier caliper whereby measurements on the lateral and major veins were avoided (White and Montes-R, 2005;

England and Attiwill, 2006). The leaf thickness was only determined for control samples in order to avoid contamination of the vernier caliper and additional leaf samples.

The leaf area was determined for each leaf by a digital image processed in *imageJ* software (O'Neal *et al.*, 2002; Abràmoff *et al.*, 2004; Easlon and Bloom, 2014).

The water content of each leaf was calculated as a percentage of fresh leaf weight according to the formula of Lichtenthaler *et al.* (2007):

$$water \quad content[\%] = [(FW - DW)/FW] * 100, \tag{1}$$

whereby the fresh leaves were weighed for fresh weight (FW), freeze-dried overnight (-80°C, 0.7-0.8 mbar) and weighted for dry weight (DW).

2.5 Analysis of C, N and stable carbon isotope (δ^{13}C)

Dried leaves were manually crushed using a mortar and pestle. An aliquot of 0.9-1.1 mg of crushed leaf material was analysed for total carbon, total nitrogen and δ^{13}C values with a Thermo Fisher Scientific Elemental Analyser coupled to a Delta V isotope mass spectrometer. Isotope values (δ^{13}C) are presented in per mil (‰) relative to the Vienna Pee Dee Belemnite (VPDB) standard.

The amount of assimilated ^{13}C during the $^{13}CO_2$ pulse-chase labelling experiment is noted as ^{13}C-excess (Srivastava *et al.*, 2017) and expressed as ^{13}C atom% (Epron *et al.*, 2012). The added ^{13}C ($\delta^{13}C_A$) was calculated as a percentage of the total ^{13}C ($\delta^{13}C_T$) using the following equation of Bahn *et al.* (2013):

$$\delta^{13}C - excess[\%] = [(100/\delta^{13}C_T) * \delta^{13}C_A] - 100 \tag{2}$$

2.6 Lipid extraction and analysis

Leaf waxes were extracted and separated into epicuticular and intracuticular lipids (**Step 1**). Separation into their constituent lipid classes was based on the polar properties of the individual lipid components (**Step 2**, **Step 3**) followed by preparation for GC analysis (**Step 4**). The method was performed as described in Wiesenberg and Gocke (2017), who provide a detailed guideline for lipid analysis. A schematic overview of the lipid extraction and separation steps are summarized in Figure 3.

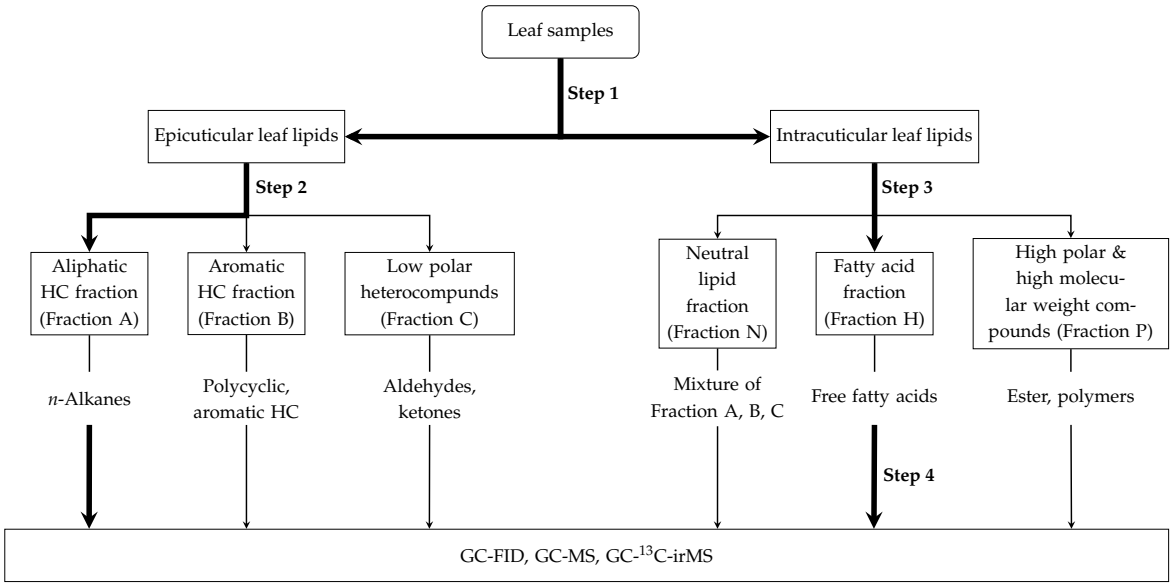

Figure 3: Schematic overview of lipid extraction and separation whereby bold arrows correspond to the extraction and analysis steps within this study (modified after Desalme et al., 2017; Wiesenberg and Gocke, 2017). *HC* = hydrocarbon

Step 1

Epicuticular lipids were extracted by dipping entire and intact leaf samples into a solvent mixture of DCM: MeOH (99:1, v/v) which was then evaporated using a rotary evaporator and filtrated over sodium sulphate (Na_2SO_4). Afterwards, total lipid extracts (TLE) were evaporated until dryness and weighed. Intracuticular lipids were extracted using an aliquot of ~150mg of crushed leaf material with 1-2ml solvent mixture of DCM:MeOH (93:7, v/v), followed by centrifugation at 800*g* for 2 minutes. The supernatant was collected and evaporated until dryness.

Step 2

The epicuticular lipids of the TLE of **Step 1** were separated into three fractions using 1.5-2.0 g activated silica gel (SiO_2, 100Å) in a 6ml glass column. The aliphatic hydrocarbons (HC; Fraction A) were eluted with 4-5ml *n*-hexane (GC *grade*), aromatic HC (Fraction B) were eluted with 5ml of solvent mixture *n*-hexane(GC *grade*):DCM (GC *grade*) (1:1, v/v) and low polar heterocompounds (Fraction C) were eluted with 4ml of solvent mixture DCM(GC *grade*):MeOH(GC *grade*) (93:7, v/v). Fraction A and B were combined to the *n*-alkane fraction due to an incomplete separation.

Step 3

The intracuticular lipids of the TLE of **Step 1** were separated into three fractions using 1.5-2.0 g KOH-coated silica gel in a 6ml glass column. Neutral lipids (Fraction N) were eluted with 30ml DCM (GC *grade*), fatty acids (Fraction H) were eluted with 20ml of solvent mixture DCM (GC *grade*):formic acid (*high purity*) (99:1, v/v) and high polar and high molecular weight compounds (Fraction P) were eluted with 4ml of solvent mixture DCM (GC*grade*):MeOH (GC *grade*) (1:1, v/v).

Step 4

Free fatty acids were further dissolved in 300μl DCM (GC *grade*) and methylated with 500μl of boron trifluorid/methanol (BF_3-CH_3OH).

2.7 *n*-Alkane identification and quantification

n-Alkanes were determined using a gas chromatography-mass spectrometer (GC-MS) and a gas chromatography-flame ionization detector (GC-FID). Measurements were performed at 70°C splitless mode at a concentration of 10-20μg/μl with injection of 1μl. Oven and injector temperatures were increased to 320°C at a rate of 10°C/ min until 120°C and 5°C/min until 320°C. Helium gas (He) was used as carrier gas (Wiesenberg and Gocke, 2017).

For the quantification of *n*-alkanes, 50μl of $D_{50}C_{24}$ (0.1mg/ml) were added to 100μl of each sample as internal standard. The concentration of *n*-alkanes was normalized by the standard and mass of dry leaf.

The average chain length (ACL; Eq. 3) as well as the carbon preference index (CPI; Eq.4) were calculated according to the equations defined by Wiesenberg and Gocke (2017):

$$ACL = \sum(z_n * n) / \sum z_n \tag{3}$$

Whereby z_n is the concentration of the respective compound and n is the number of carbon atoms.

$$CPI = [(\sum C_{25} - C_{33odd} / \sum C_{24} - C_{30even}) + (\sum C_{25} - C_{33odd} / \sum C_{26} - C_{32even})]/2 \tag{4}$$

2.8 *n*-Alkane δ^{13}C analysis

The *n*-alkane stable carbon isotope composition was assigned using gas chromatography carbon isotope mass spectrometry (GC-C-irMS). GC conditions were identical as above. The δ^{13}C values were presented in per mil (‰) according to the VPDB standard. Each sample (900μl) was measured three times with an alkane mix (C_{20}, C_{24}, C_{30}) as external standard. The ^{13}C-excess was calculated using Eq.2.

Fatty acids (100μl) were measured three times with $D_{39}C_{20}$ acid (0.1mg/ml; 50μl) as internal and with alkane mix (C_{20}, C_{24}, C_{30}) as external standard.

2.9 Statistical analysis

Leaf samples of all spots (n=8) were used to analyse physical leaf properties, total carbon and total nitrogen concentrations, δ^{13}C values of bulk tissues and epicuticular wax content. Thereby significant differences between sun-exposed and shaded leaves were tested using a Student's t-test ($p < 0.05$). The δ^{13}C values were additionally tested using a Student's t-test ($p < 0.05$) for the difference between leaves collected from the topmost and the terminal part of the same branch. Measurements of physical leaf properties and carbon and nitrogen concentrations were normalized by dry leaf weight (dry wt). In all figures and tables, average values $\pm$ sd are presented where average values $\pm$ sd consist of 8 samples of the same sampling date.

For the *n*-alkane composition and stable carbon (δ^{13}C) isotope composition of two spots at each site including control (n=4) were used. *n*-Alkane composition were only tested for significant differences between sun-exposed and shaded canopy positions using a Student's t-test ($p < 0.05$) due to no significant differences between control and labelled leaf samples ($p > 0.05$). Data for compound specific δ^{13}C values were tested using a Student's t-test and one-way ANOVA ($p < 0.05$). Values of *n*-alkane composition as well as compound specific δ^{13}C values were normalized by dry leaf weight (dry wt) and leaf unit area. All lipid fractions were measured three times to ensure reproducibility. Hence, in all figures and tables average values $\pm$ sd equals to 3 analytical measurement runs; difference between analytical measurements did not exceed 1‰; outliers were not considered (n=9). All statistical analyses and visualizations were performed with R studio software 1.1.383 (RStudio Team, 2016).

3 Results

3.1 Physical leaf properties

3.1.1 SPAD values

A higher chlorophyll concentration (+4%, $p > 0.05$) was observed in early August (Day of the year (DOY) 221) in sun-exposed leaves (35.43 $\pm$ 0.9) than in shaded leaves (33.98 $\pm$ 0.5). However, seen over the entire sampling period, chlorophyll content did not differ significantly ($p > 0.05$). Both sun-exposed and shaded leaves exhibited greatest chlorophyll concentrations in early August (DOY 221) and lowest in the late end of the growing season in early October (DOY 284). Subsequently, chlorophyll concentration of sun-exposed leaves decreased continuously until early October with a SPAD value of 26.0 $\pm$ 2.4. Controversially, chlorophyll concentration in shaded leaves increased (3%) between mid and late August (DOY 235-242) with a SPAD value of 32.5 $\pm$ 0.3, followed by continuously decreasing values to 28.9 $\pm$ 0.2 as the growing season proceeded. Overall, SPAD values of shaded leaves ranged between 28.9 and 33.9 with an average value of 31.8 $\pm$ 1.8. Similar SPAD values were measured for sun-exposed leaves with values between 26.0 and 35.4 and an average value of 31.7 $\pm$ 4.2 (Figure 4).

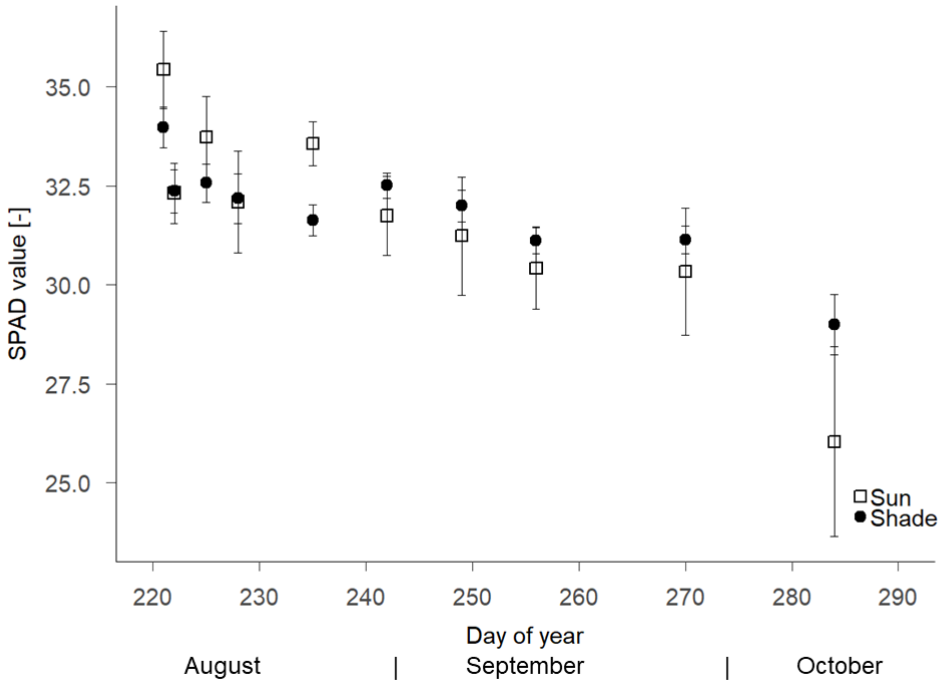

Figure 4: SPAD values (n=8 $\pm$ sd) of sun-exposed and shaded leaves throughout the late growing season (Aug - Oct, 2018).

3.1.2 Leaf thickness and leaf area

Sun-exposed leaves are characterized by a larger leaf thickness (+30%; $p < 0.05$) in comparison to shaded leaves. Sun-exposed leaves exhibited a leaf thickness between 32.50 and 55.00 μm and an average leaf thickness of 44.16 $\pm$ 8.12 μm whereby the leaf thickness of shaded leaves ranged between 16.75 and 50.00 μm with an average leaf thickness of 33.02 $\pm$ 12.54 μm. While shaded leaves reached their maximum leaf thickness of 50.00 μm in early August (DOY 221), sun-exposed leaves reached their maximum leaf thickness of 55.00 μm in late August (DOY 235). Moreover, while shaded leaves became thicker again in early October (DOY 284; 22.50 μm), sun-exposed leaves showed a steady decline in leaf thickness over the late growing season. Nevertheless, when compared to the leaf thickness in early August, both showed a decline (sun-exposed leaves: -20%; shaded leaves: -55%) in leaf thickness as the growing season proceeded (Figure 5).

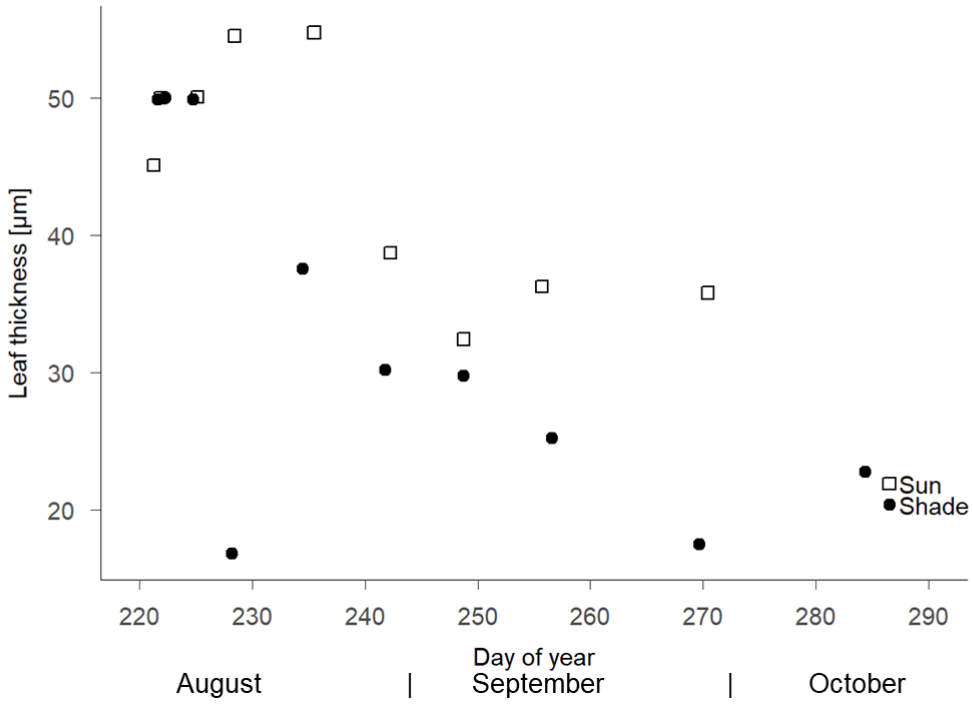

Figure 5: Leaf thickness of sun-exposed and shaded leaves throughout the late growing season (Aug - Oct, 2018). Each data point represents the leaf thickness of a single leaf of sun-exposed and shaded leaves. The leaf thickness of the sun-exposed leaf in early October (DOY 284) could not be measured due to a damaged leaf sample.

A clearly larger leaf area (+20%; $p < 0.05$) was observed in shaded leaves over sun-exposed leaves. Leaf area of shaded leaves ranged between 33.98 and 78.63 cm^2 with an average leaf area of 53.11 $\pm$ 20.4 cm^2 while leaf area of sun-exposed leaves varied between 33.62 and 54.02 cm^2 with an average leaf area of 41.56 $\pm$ 15.6 cm^2. Maximum leaf size of shaded leaves was measured in early August (DOY 221) with a leaf area of 78.63 $\pm$ 6.5 cm^2 followed by a second maximum (+20%) in mid-September (DOY 256) with a leaf area of 44.47 $\pm$ 7.4 cm^2. Subsequently, leaf area of shaded leaves

was smaller (-55%; 33.9 $\pm$ 9.1 cm^2) as growing season proceeded relative to the initial leaf size in early August. The opposite was observed in sun-exposed leaves with smallest leaves in early August (DOY 222) with a leaf area of 33.62 $\pm$ 4.6 cm^2 and largest leaves in late September (DOY 270) with a leaf area 54.02 $\pm$ 9.5 cm^2 (Figure 6).

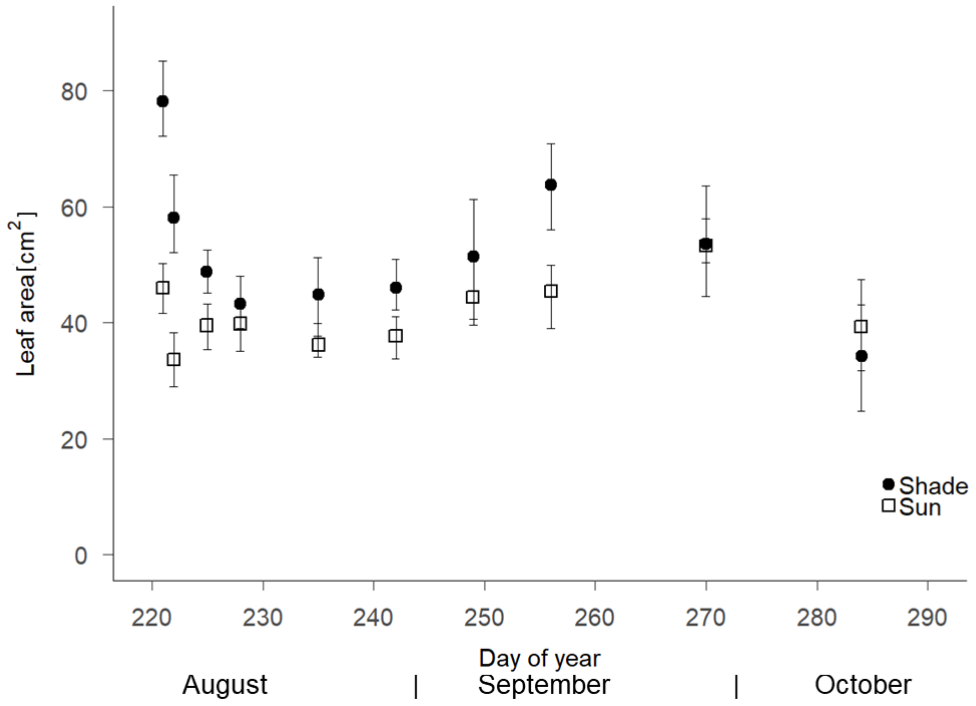

Figure 6: Variability in leaf area of sun-exposed and shaded leaves (n=8 $\pm$ sd) throughout the late growing season (Aug - Oct, 2018).

3.1.3 Water content

A significantly greater water content (+10%; $p < 0.0001$) was observed in shaded leaves than in sun-exposed leaves with an average water content of 57.67 $\pm$ 1.3 mg g^{-1} and 51.71 $\pm$ 4.75 mg g^{-1} in shaded and sun-exposed leaves, respectively. The highest water content was observed in shaded leaves in early August (DOY 222) with 59.56 $\pm$ 0.7 mg g^{-1}, followed by a slight decrease (DOY 225; -5%) to a water content of 56.67 $\pm$ 0.8 mg g^{-1}. Afterwards, during the remaining growing season, the water content remained relatively constant in shaded leaves (DOY 284; 57.30 $\pm$ 0.9 mg g^{-1}). In contrast, a rather wide fluctuation in water content throughout the late growing season was observed in sun-exposed leaves with a maximum water content of 54.57 $\pm$ 2.1 mg g^{-1} in mid-September (DOY 256) and a decrease in water content as the growing season proceeded (DOY 284; 51.04 $\pm$ 1.6 mg g^{-1}; Figure 7).

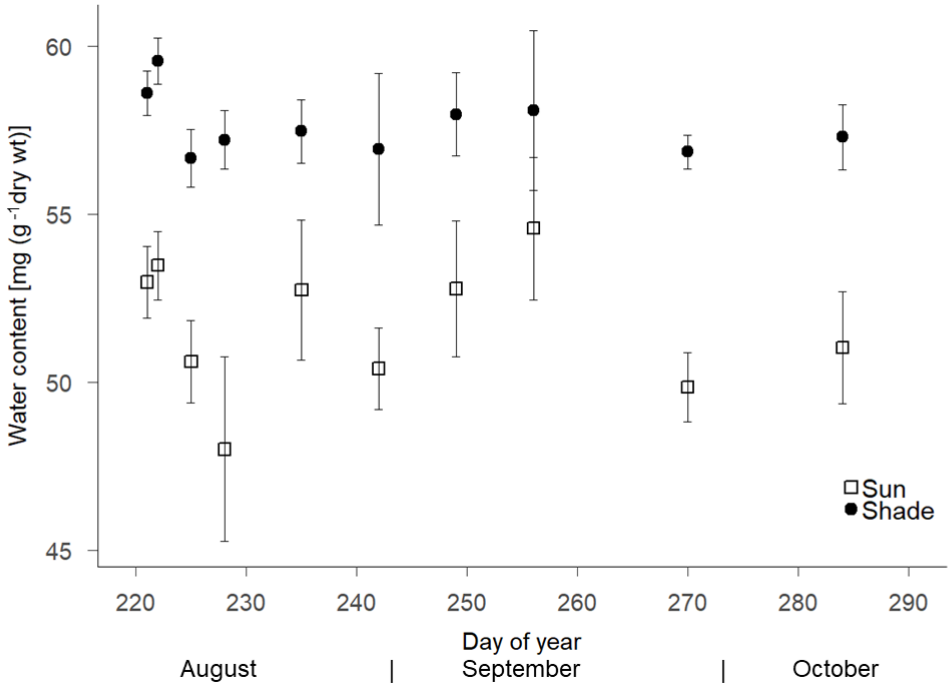

Figure 7: Variability in water content of sun-exposed and shaded leaves (n=8 ± sd) during the late growing season (Aug - Oct, 2018).

3.2 C and N concentrations

Total carbon (TC) concentration in sun-exposed leaves was clearly higher (+4%; $p < 0.0001$) than in shaded leaves with an average total carbon concentration of 46.24 ± 1.3 mg g^{-1} and 44.42 ± 1.7 mg g^{-1} in sun-exposed and shaded leaves, respectively. A rapid increase in TC concentration was observed in both sun-exposed (+3%) and shaded leaves (+4%) in early August (DOY 221-228) with a TC concentration of 46.06 ± 0.5 mg g^{-1} in sun-exposed and 44.51 ± 0.3 mg g^{-1} in shaded leaves. Moreover, TC concentration steadily increased as the growing season proceeded to a TC concentration of 47.36 ± 0.5 mg g^{-1} in sun-exposed leaves and to 45.09 ± 0.3 mg g^{-1} in shaded leaves. Consequently, a larger TC concentration was observed in early October (DOY 284) in sun-exposed (+3%) and shaded leaves (+5%) when compared to the initial TC concentration measured in early August (Figure 8).

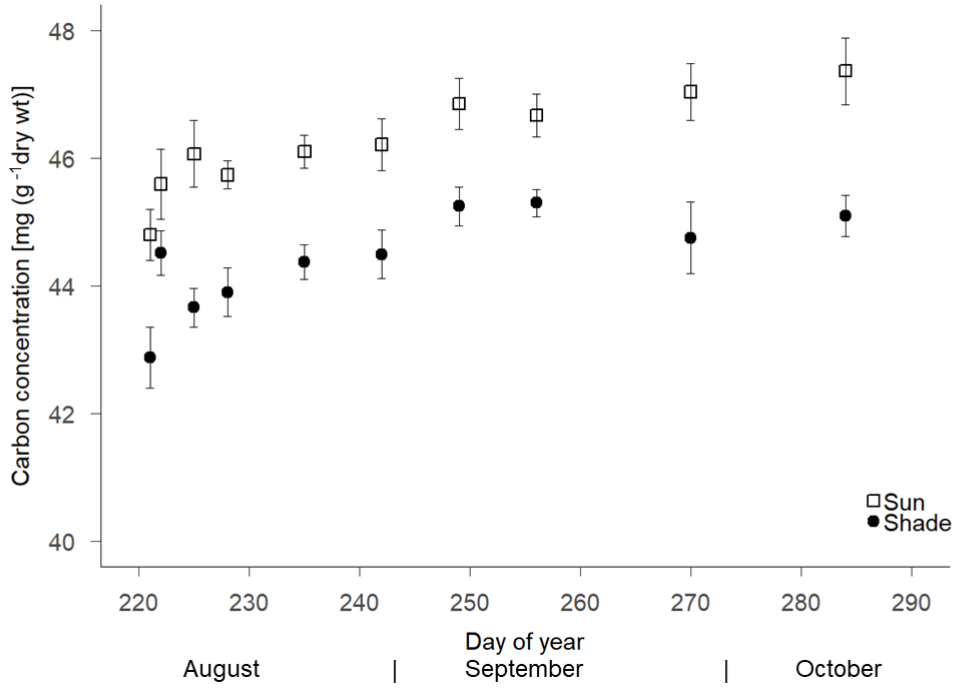

Figure 8: Variability in the total carbon (TC) concentration of sun-exposed and shaded leaves (n=8 ± sd) throughout the late growing season (Aug - Oct, 2018).

A significantly greater total nitrogen (TN) concentration (+15%; $p < 0.0001$) was observed in shaded over sun-exposed leaves with an average total nitrogen concentration of 2.02 ± 0.1 mg g^{-1} in shaded and 1.73 ± 0.3 mg g^{-1} in sun-exposed leaves, respectively. Moreover, shaded leaves reached a maximum TN concentration of 2.17 ± 0.04 mg g^{-1} in early August (DOY 222) followed by a second increase in mid-September (DOY 256) with a TN of 2.11 ± 0.05 mg g^{-1}. Subsequently, TN concentration continuously decreased (-4%) as growing season proceeded to a TN concentration of 1.97 ± 0.03 mg g^{-1}. On the other hand, sun-exposed leaves reached a maximum TN concentration of 1.97 ± 0.07 mg g^{-1} in late August (DOY 235), followed by a second increase in mid-September (DOY 256; 1.76 ± 0.13 mg g^{-1}). Overall, TN concentration decreased in both sun-exposed and shaded leaves as the growing season proceeded (Figure 9).

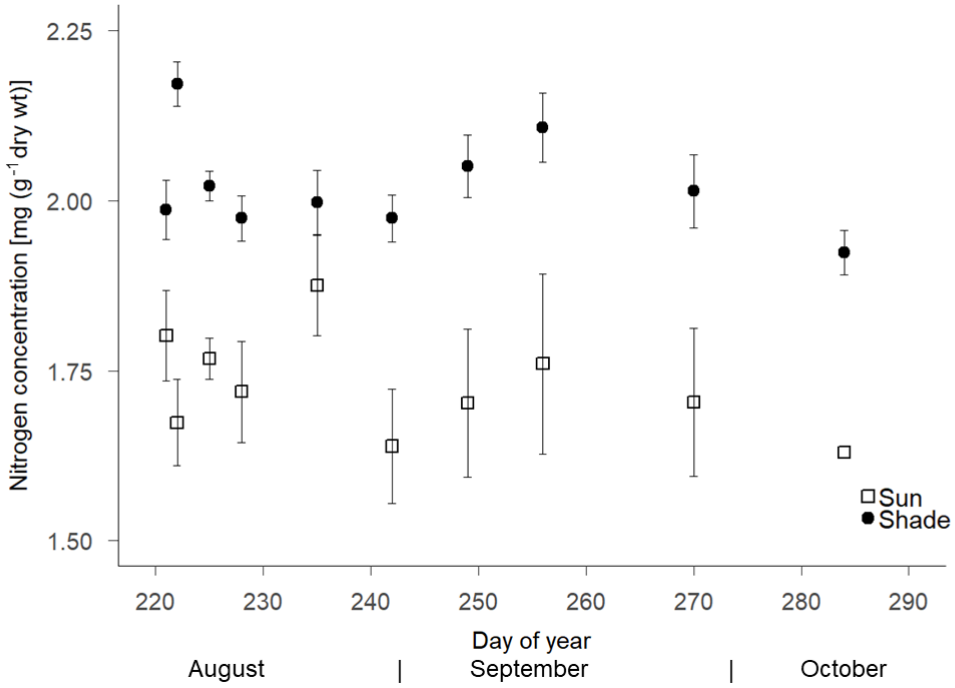

Figure 9: Variability in the total nitrogen (TN) concentration of sun-exposed and shaded leaves (n=8 ± sd) throughout the late growing season (Aug - Oct, 2018).

The C:N ratio reflects the TC and TN concentrations that resulted in an increased (+25%; $p < 0.0001$) C:N ratio from shaded to sun-exposed leaves with average values of 22.04 ± 1.3 and 27.66 ± 6.09. Lowest C:N ratios were observed in early August (DOY 221 and 222) with 25.09 ± 0.88 and 20.53 ± 0.34 and greatest C:N ratios were observed in early October (DOY 284) with 32.14 ± 4.6 and 23.45 ± 0.3 within sun-exposed and shaded leaves (Figure 10). Table 1 provides an overview of leaf properties (For more detailed data, see Supplementary Tables I and II)

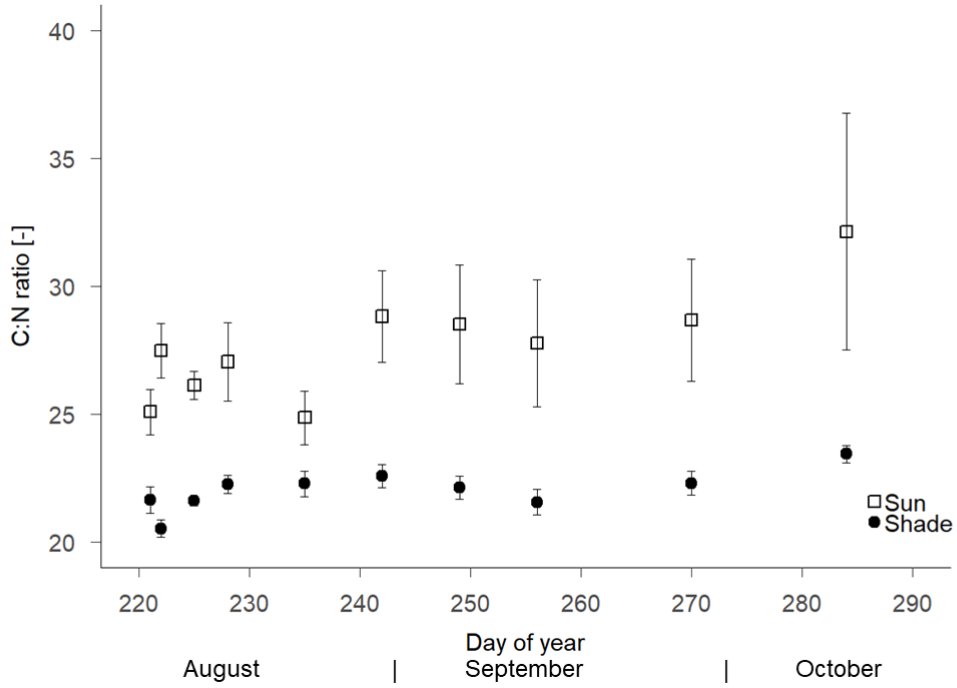

Figure 10: Variability in the C:N ratio of sun-exposed and shaded leaves (n=8 ± sd) throughout the late growing season (Aug - Oct, 2018).

Table 1: Summary of physical leaf properties. The average values ± sd represent 80 samples for sun-exposed and shaded leaves. With the exception of the leaf thickness, which was only measured for control leaf samples and thus represents the average value ± sd of 20 samples for sun-exposed and shaded leaves.
*, $p < 0.05$; **, $p < 0.01$; ***, $p < 0.001$; ****, $p < 0.0001$; ns, not significant

Physical leaf properties	**Shaded leaves**	**Sun-exposed leaves**
SPAD value [-]	31.80 ± 1.8^{ns}	31.70 ± 4.2^{ns}
Leaf thicknesss [μm]	$33.03 \pm 12.5^{*}$	$44.17 \pm 8.1^{*}$
Leaf area [cm^2]	$53.11 \pm 20.4^{*}$	$41.56 \pm 15.6^{*}$
Dry leaf weight [mg]	$137.64 \pm 56.7^{****}$	$214.23 \pm 67.6^{****}$
Water content [mg g^{-1}]	$57.67 \pm 1.3^{****}$	$51.71 \pm 4.7^{****}$
TC concentration [mg g^{-1}]	$44.42 \pm 1.7^{****}$	$46.24 \pm 1.3^{****}$
TN concentration [mg g^{-1}]	$2.02 \pm 0.1^{****}$	$1.73 \pm 0.3^{****}$
C:N ratio	$22.04 \pm 1.3^{****}$	$27.66 \pm 6.1^{****}$

3.3 Epicuticular wax content

Epicuticular wax content per dry leaf weight was significantly larger (+15%; $p < 0.001$) in shaded than in sun-exposed leaves with an average epicuticular wax content of 6.9 $\pm$ 1.5 mg g^{-1} and 5.8 $\pm$ 0.8 mg g^{-1}. Epicuticular wax content per dry leaf weight in shaded leaves ranged between 6.19 and 8.11 mg g^{-1} while epicuticular wax content per dry leaf weight in sun-exposed leaves ranged between 5.18 and 6.81 mg g^{-1}. An increased epicuticular wax content was observed in both sun-exposed and shaded leaves in early August (DOY 221-228) with values up to 6.81 $\pm$ 0.1 mg g^{-1} and 7.98 $\pm$ 1.1 mg g^{-1}. Subsequently, epicuticular wax content per dry leaf weight continuously decreased in sun-exposed leaves until early October (DOY 284) with a 10% lower epicuticular wax content (5.18 $\pm$ 0.4 mg g^{-1}) when compared to the initial amount in early August. Inversely, an increased epicuticular wax content per dry leaf weight was observed in shaded leaves between late September (7.04 $\pm$ 0.7 mg g^{-1}) and early October (8.11 $\pm$ 1.3 mg g^{-1}). This results in a 20% larger epicuticular wax content per dry leaf weight towards the late end of growing season as compared to the initial epicuticular wax content in early August (Figure 11).

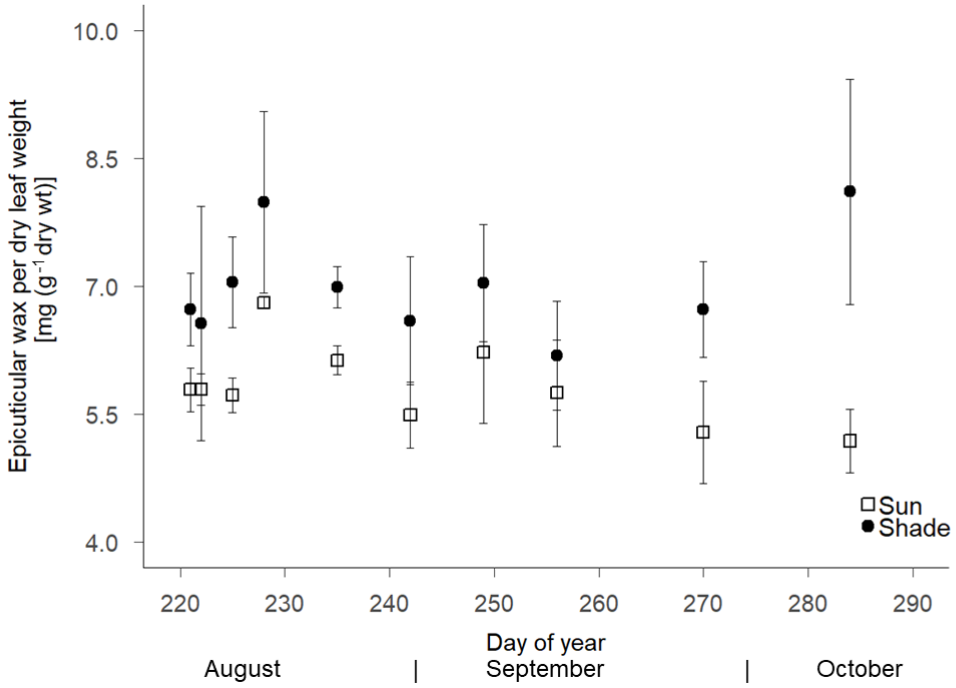

Figure 11: Variability in the epicuticular wax content normalized by dry leaf weight of sun-exposed and shaded leaves (n=8 $\pm$ sd) throughout the late growing season (Aug - Oct, 2018).

On the other hand, epicuticular wax content per leaf unit area was significantly larger (+45% $p < 0.0001$) in sun-exposed than in shaded leaves. Average epicuticular wax content per leaf unit area in sun-exposed leaves was 36.74 $\pm$ 8.4 μg cm^{-2} whereas the average epicuticular wax content per leaf unit area in shaded leaves was 19.77 $\pm$ 3.8 μg cm^{-2}. An increased epicuticular wax content per leaf

unit area was observed in both sun-exposed and shaded leaves in early August (DOY 221-228) with 23.85 $\pm$ 1.1 μg cm^{-2} in shaded and 43.88 $\pm$ 6.5 μg cm^{-2} in sun-exposed leaves. A second increase was observed in shaded leaves between early September (DOY 256; 18.06 $\pm$ 1.3 μg cm^{-2}) and October (DOY 284; 21.84 $\pm$ 3.1 μg cm^{-2}). In contrast, a second increase was observed in sun-exposed leaves in late September (DOY 270) with an average of 41.01 $\pm$ 2.7 μg cm^{-2} followed by a sharp decline to 30.05 $\pm$ 4.3 μg cm^{-2} in early October. Overall, sun-exposed leaves showed a decline in epicuticular wax content per leaf unit area (-10%) as the growing season proceeded whereas shaded leaves showed an increased (+30%) epicuticular wax content per leaf unit area towards the end of the growing season in comparison to their initial wax content in early August (Figure 12).

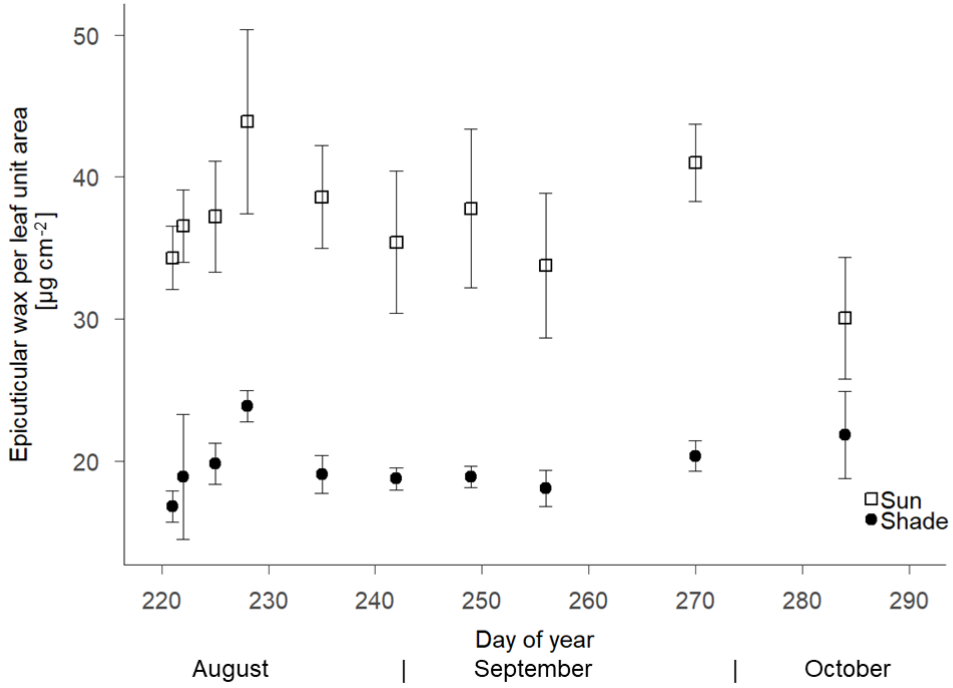

Figure 12: Variability in the epicuticular wax content normalized by leaf unit area of sun-exposed and shaded leaves (n=4 $\pm$ sd) throughout the late growing season (Aug - Oct, 2018). The large deviations in sun-exposed leaves are due to the large variability in the epicuticular wax content within the leaf samples.

3.4 *n*-Alkane composition

n-Alkane content

There was no significant difference in the *n*-alkane content per dry leaf weight ($p > 0.05$) in sun-exposed and shaded leaves. *n*-Alkane content in shaded leaves ranged between 1.62 and 2.87 mg g^{-1} with an average content of 2.01 $\pm$ 0.2 mg g^{-1} while *n*-alkane content in sun-exposed leaves ranged between 1.66 and 2.52 mg g^{-1} with an average content of 2.1 $\pm$ 0.3 mg g^{-1}. Shaded leaves

showed an increased *n*-alkane content (2.07 $\pm$ 0.3 mg g^{-1}) in the late end of the growing season (DOY 256-284) in comparison to shaded leaves (Figure 13).

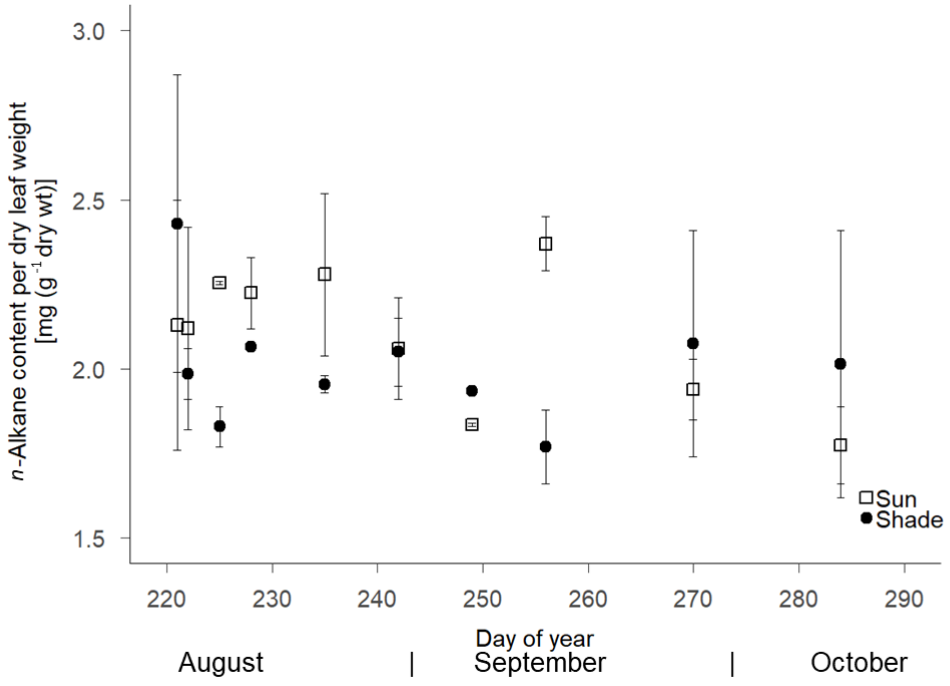

Figure 13: Variability in the *n*-alkane content normalized by dry leaf weight of sun-exposed and shaded leaves (n = 2 $\pm$ sd) throughout the late growing season (Aug - Oct, 2018). The large deviations are due to the large variability in dry leaf weight within the leaf samples.

In contrast, the *n*-alkane content per leaf unit area was significantly higher in sun-exposed ($p < 0.0001$) than in shaded leaves with an average *n*-alkane content of 13.38 $\pm$ 3.0 μg cm^{-2} in sun-exposed and 5.24 $\pm$ 0.8 μg cm^{-2} in shaded leaves. Furthermore, while the *n*-alkane content in shaded leaves remained relatively constant throughout the late growing season, *n*-alkane content in sun-exposed leaves was highly dynamic throughout the late growing season. An increased *n*-alkane content was observed in sun-exposed leaves in early August (DOY 221-228) with an *n*-alkane content of 15.14 $\pm$ 1.5 μg cm^{-2}. Afterwards, the *n*-alkane content remained relatively constant until the late end of the growing season (DOY 284) with a decreasing *n*-alkane content, especially in sun-exposed leaves (9.78 $\pm$ 1.6 μg cm^{-2}; Figure 14; Supplementary Tables III and IV provide a summary of the epicuticular wax and *n*-alkane content of sun-exposed and shaded leaves).

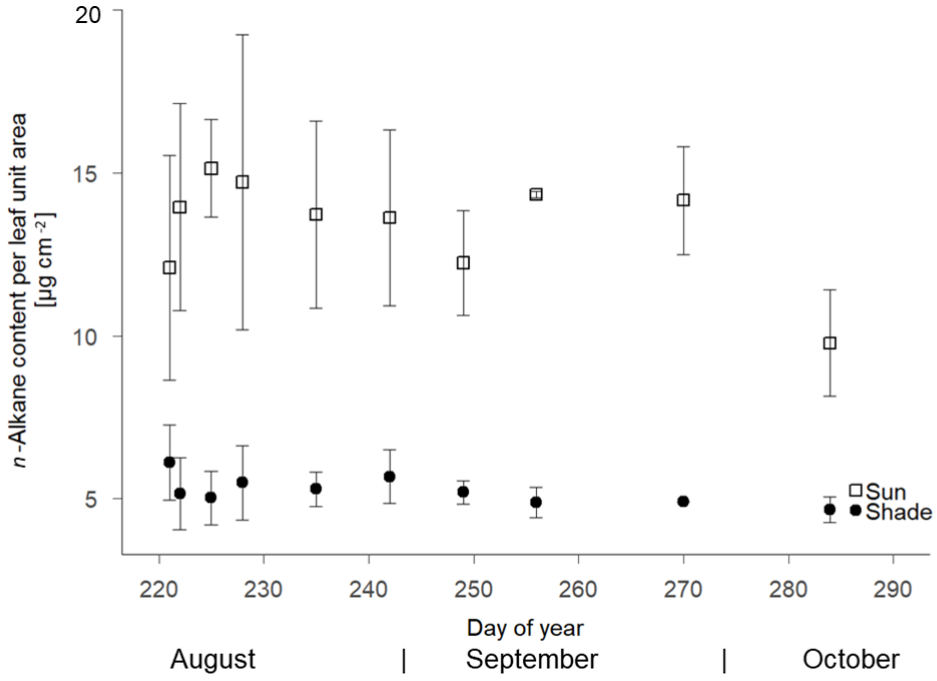

Figure 14: Variability in the *n*-alkane content normalized by leaf unit area of sun-exposed and shaded leaves (n = 2± sd) throughout the late growing season (Aug - Oct, 2018).

In all investigated leaf samples, *n*-alkanes showed a strong odd-over-even predominance with numbers of extractable *n*-alkanes between C_{22} to C_{32}, whereby C_{25}, C_{27} and C_{29} were the most abundant. Particularly an exclusive production (90%) of C_{27} was observed in both sun-exposed and shaded leaves with a slightly higher concentration in sun-exposed (+2%) than in shaded leaves (Supplementary Figure II). A higher concentration of *n*-C_{25} and C_{29} has been measured in shaded leaves (2.5 % and 5.5%) than in sun-exposed leaves (3.1% and 3.5%). Hence, shaded leaves showed a significantly higher higher C_{29}/C_{25} ratio (2.2) as opposed to sun-exposed leaves (1.1; Figure 15).

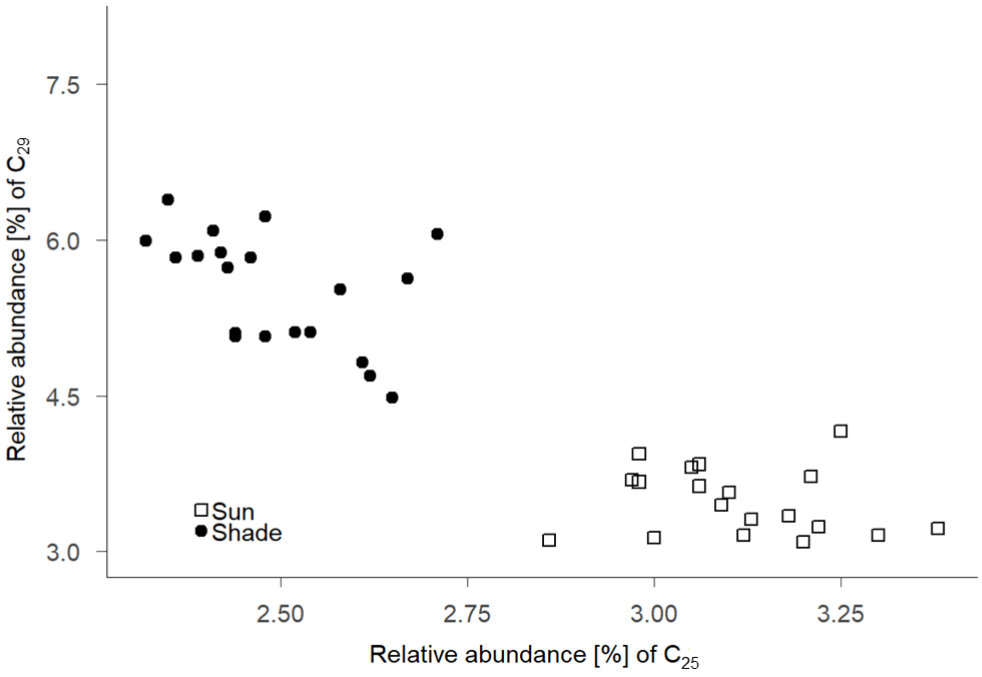

Figure 15: Relative abundance of C_{25} and C_{29} *n*-alkane of sun-exposed and shaded leaves (n = 20).

Although sun-exposed leaves had a higher concentration of *n*-alkanes (+60%; $p < 0.0001$) compared to shaded leaves, *n*-alkanes of shaded leaves had a clearly ($p < 0.0001$) longer chain length in contrast to sun-exposed *n*-alkanes. Thus, the average chain length (ACL) of shaded leaves ranged between 27.03 and 27.11 with an average of 27.06 ± 0.02, whereas ACL values of sun-exposed leaves ranged between 26.96 and 27.01 with an average of 26.99 ± 0.01. Likewise, the carbon preference index (CPI) of shaded leaves was significantly larger ($p < 0.01$) with an average value of 70.72 ± 5.3 as opposed to sun-exposed leaves with an average CPI value of 63.65 ± 15.3 (Figures 16 a and b).

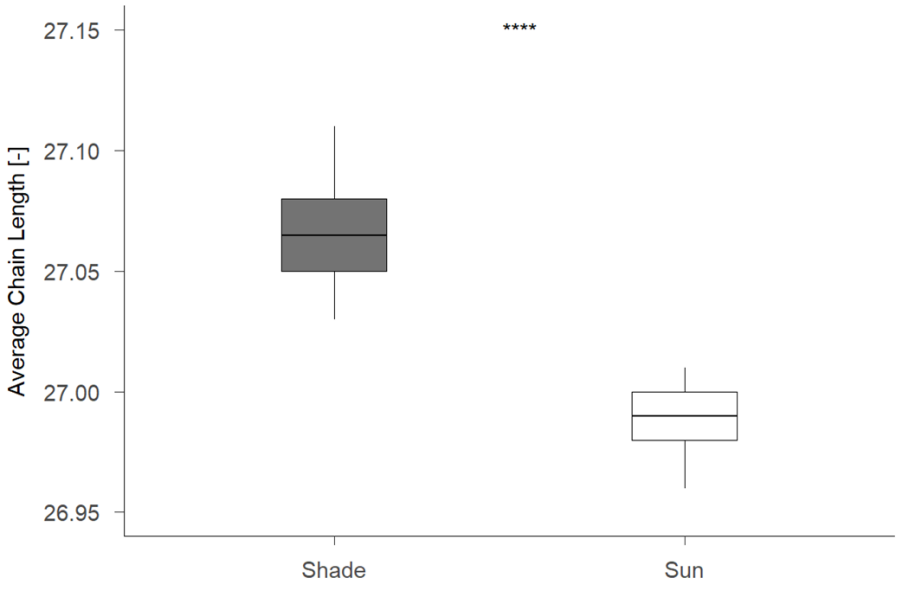

(a) Average chain length (ACL) of sun-exposed and shaded leaves.

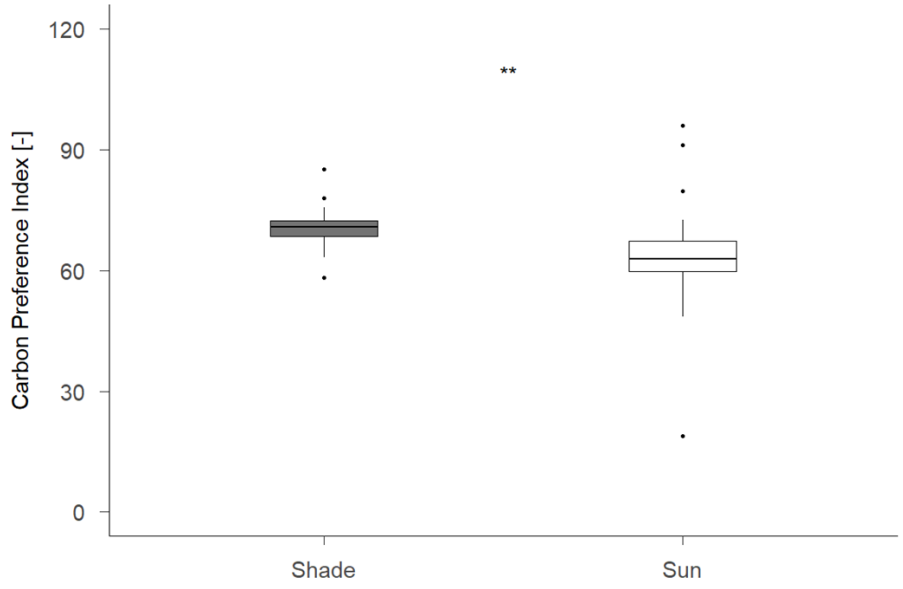

(b) Carbon preference index (CPI) of sun-exposed and shaded leaves.

Figure 16: Average chain length (ACL) and carbon preference index (CPI) of sun-exposed and shaded leaves. Each box represents the values of 20 samples for sun-exposed and shaded leaves. **, $p < 0.01$; ****, $p < 0.0001$.

Slight fluctuations in ACL and CPI values of sun-exposed and shaded leaves were observed throughout the late growing season with a minor fluctuation in sun-exposed leaves. Additionally, while ACL values of shaded leaves decreased (-2%; 27.05 ± 0.01) in early October (DOY 284), ACL values of sun-exposed leaves remained relatively constant with an ACL of 26.99 ± 0.001 throughout the late growing season (Figure 17 a). In contrast, while CPI values of shaded leaves remained rel-

atively constant throughout the late growing season, sun-exposed leaves showed a wide variability in CPI values during the late growing season (Figure 17 b).

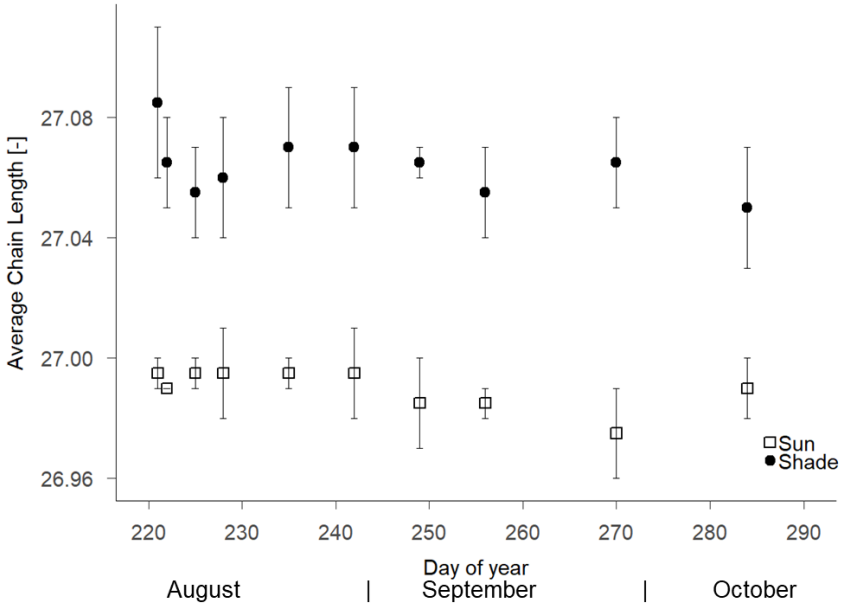

(a) Variability in the ACL values of sun-exposed and shaded *n*-alkanes throughout the late growing season.

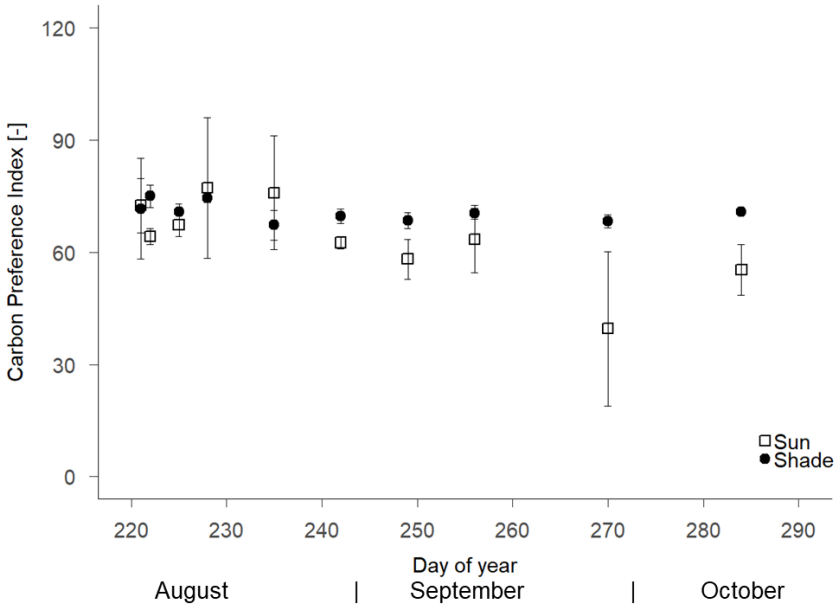

(b) Variability in the CPI values of sun-exposed and shaded *n*-alkanes throughout the late growing season.

Figure 17: Variability in the ACL and CPI values of *n*-alkanes of sun-exposed and shaded leaves (n=2 $\pm$ sd) throughout the late growing season (Aug - Oct, 2018).

3.5 Stable carbon isotope (δ^{13}C) values

Control samples of sun-exposed leaves exhibited an enrichment in δ^{13}C of 5% (+1.5 ‰; $p < 0.0001$) in contrast to the control samples of shaded leaves. An average δ^{13}C value of -30.18 ± 0.18 ‰ was observed in sun-exposed leaves with values between -30.42 and -29.73 ‰. In contrast, the average δ^{13}C of -31.64 ± 0.22 ‰ in shaded leaves was slightly lighter with δ^{13}C values between -32.15 and -31.29 ‰ (Figure 18).

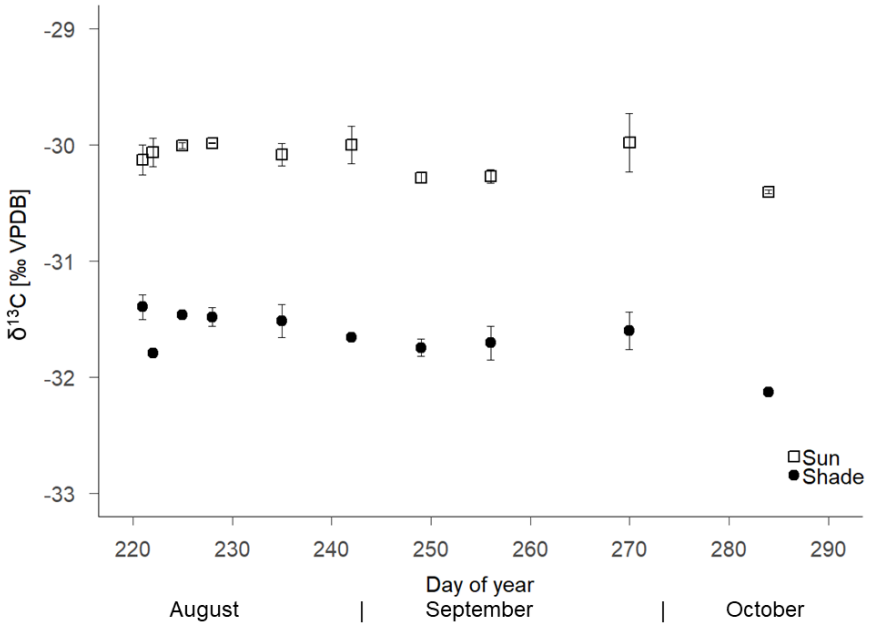

Figure 18: Variability in δ^{13}C values of bulk tissue of control samples of sun-exposed and shaded leaves (n=2) throughout the late growing season (Aug - Oct, 2018). The average value ± sd represents three measurement runs.

No significant difference in δ^{13}C values ($p > 0.05$) was observed between leaves from the topmost and the terminal part of the same branch, neither in sun-exposed nor shaded leaves. Shaded leaves from the topmost parts had an average δ^{13}C value of -31.67 ± 0.2‰, while leaves collected from the terminal parts had an average δ^{13}C value of -31.62 ± 0.2‰. Similar observations were made for sun-exposed leaves collected from the topmost and the terminal part of the same branch with average δ^{13}C values of 30.08 ± 0.2‰ and -30.13 ± 0.2‰ (Supplementary Figures III a and b).

The δ^{13}C values of shaded *n*-alkanes ranged between -34.76 and -33.28 ‰ with an average δ^{13}C value of -34.28 ± 0.20 ‰, whereas ^{13}C values of sun-exposed *n*-alkanes varied between -32.06 and -30.80 ‰ with an average δ^{13}C value of -31.31 ± 0.28 ‰. Overall, *n*-alkanes of both sun-exposed and shaded leaves, were significantly depleted in δ^{13}C (1-3‰) when compared to bulk tissue (Figure 19; Supplementary Table V).

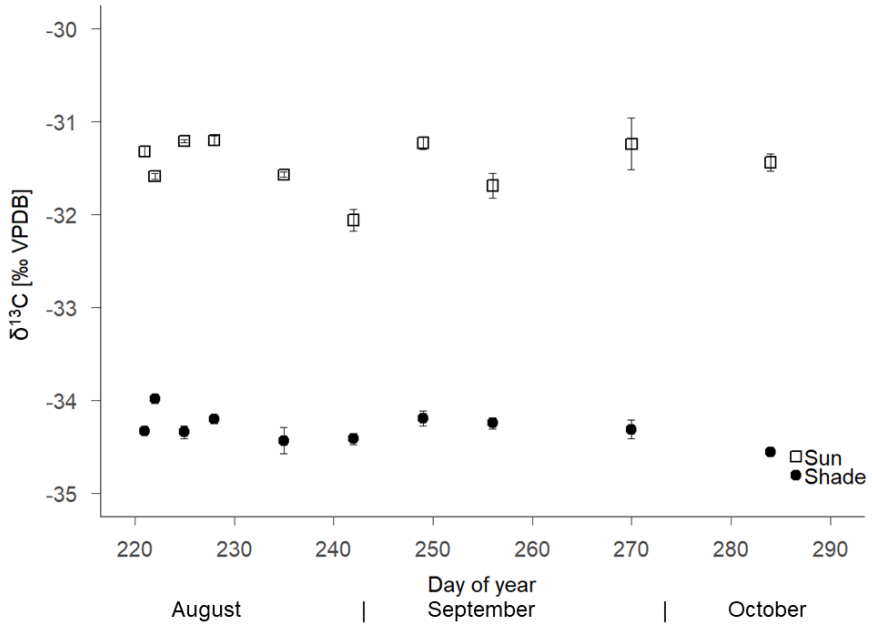

Figure 19: Variability in $\delta^{13}C$ values of *n*-alkanes of control samples of sun-exposed and shaded leaves (n=2) throughout the late growing season (Aug - Oct, 2018). The average value ± sd represents three measurement runs.

The largest enrichment in ^{13}C was observed one day after the labelling on the 10^{th} of August (DOY 222) with a ^{13}C-excess of 30.90 ± 1.77 mg g^{-1} in shaded and 19.57 ± 2.36 mg g^{-1} in sun-exposed leaves, indicating a significant assimilation of ^{13}C (+20-30%; $p < 0.0001$) as opposed to control leaves. Moreover, sun-exposed and shaded leaves displayed the same trend in ^{13}C assimilation. A first increase in ^{13}C assimilation was observed one day after the labelling and a second increase in late August (DOY 242) with a ^{13}C-excess of 3.95 ± 0.26 mg g^{-1} in sun-exposed and 9.59 ± 0.38 mg g^{-1} in shaded leaves. Although shaded leaves typically show a greater depletion in $\delta^{13}C$ than sun-exposed leaves, a greater ^{13}C assimilation (+10%;$p < 0.05$) was observed in shaded leaves compared to sun-exposed leaves (Figure 20).

The greatest ^{13}C enrichment in *n*-alkanes was observed in sun-exposed leaves with a ^{13}C-excess of 0.12 ± 0.02 mg g^{-1} four days (DOY 225) after labelling. On the other hand, *n*-alkanes of shaded leaves showed an enrichment in ^{13}C 35 days after labelling (DOY 256) with a ^{13}C-excess of 0.08 ± 0.04 mg g^{-1} (Figure 21). Therefore, a certain time lag in ^{13}C assimilation between bulk tissue and *n*-alkanes was identified with a time lag up to eight times longer in shaded leaves relative to sun-exposed leaves. Overall, a ^{13}C assimilation of approximately 20-30% was observed in bulk tissue whereof roughly 1% was assimilated in *n*-alkanes.

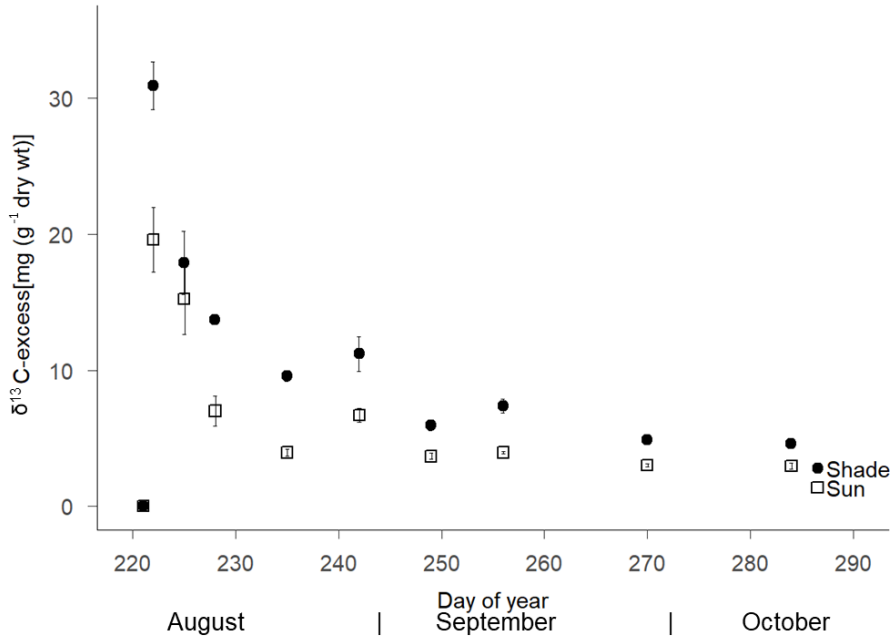

Figure 20: ^{13}C-excess of bulk tissue in sun-exposed and shaded leaves (n=8) throughout the late growing season (Aug - Oct, 2018). The average value ± sd represents three measurement runs.

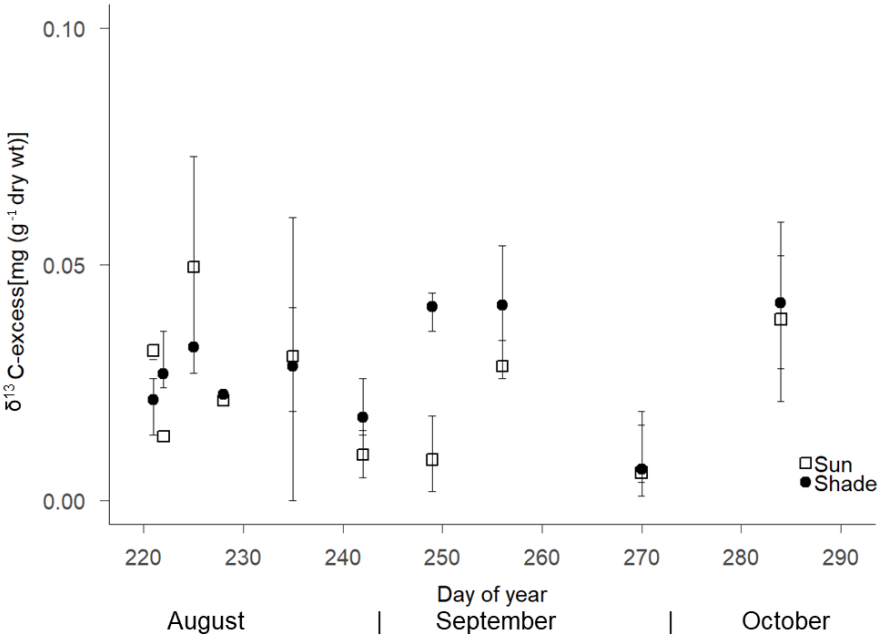

Figure 21: ^{13}C-excess of *n*-alkanes in sun-exposed and shaded leaves (n=2) throughout the late growing season (Aug - Oct, 2018). The average value ± sd represents three measurement runs. The large deviations are due to the large variability in dry leaf weight within the leaf samples.

3.6 Identification of the wax renewal rate

The time period in which the wax renewal takes place was calculated on the basis of the ^{13}C-excess of *n*-alkanes. Specifically, the time between the greatest ^{13}C-enrichment and the decline to the original δ^{13}C value was determined. While the δ^{13}C values returned to initial values within three days (DOY 225-228) in sun-exposed leaves, the δ^{13}C value of shaded leaves returned to initial values within two weeks (DOY 256-270; Figure 21; Table 2). The quantity of renewed waxes (per day) was calculated on the basis of the *n*-alkane content normalized by leaf unit area. The amount of renewed waxes was 0.8μg cm^{-2} per day in sun-exposed and 0.03 μg cm^{-2} per day in shaded leaves. This indicates a ~27 times faster wax renewal rate in sun-exposed leaves. Moreover, the quantity of renewed waxes corresponds to approximately 5% in sun-exposed and 0.5% in shaded leaves of the total epicuticular wax content. Consequently, sun-exposed leaves have not only a significantly faster wax renewal rate, but also a higher quantity (by a factor of 10) of renewed waxes in a much shorter time period as compared to shaded leaves.

Table 2: ^{13}C-excess and *n*-alkane content of sun-exposed and shaded leaves throughout the late growing season (Aug - Oct, 2018). The highlighted values indicate the *n*-alkane content normalized by leaf unit area and the ^{13}C-excess equal the initial one, which allows to determine the wax renewal rate. The values of the *n*-alkane equals one sample per date for sun-exposed and shaded leaves. Average ± sd of the ^{13}C excess equals three measurement runs.

DOY	Shaded leaves *n*-Alkane content [μg cm $^{-2}$]	Shaded leaves ^{13}C-excess [mg g^{-1}] [mg g^{-1}]	Sun-exposed leaves *n*-Alkane content [μg cm $^{-2}$]	Sun-exposed leaves ^{13}C-excess [mg g^{-1}] [mg g^{-1}]
221	7.26	0.02 ± 0.006	15.55	0.03 ± 0.000
222	6.26	0.03 ± 0.006	17.13	0.01 ± 0.046
225	5.85	0.03 ± 0.032	16.64	0.05 ± 0.023
228	6.63	0.02 ± 0.038	19.24	0.02 ± 0.038
235	5.83	0.03 ± 0.030	16.61	0.03 ± 0.011
242	6.50	0.02 ± 0.006	16.32	0.01 ± 0.005
249	5.56	0.04 ± 0.004	13.86	0.01 ± 0.008
256	5.35	0.04 ± 0.014	14.43	0.03 ± 0.004
270	4.91	0.01 ± 0.006	15.81	0.01 ± 0.009
284	5.07	0.04 ± 0.012	8.14	0.04 ± 0.019

4 Discussion

4.1 Epicuticular wax content

For the discussion of the epicuticular wax content, including *n*-alkane content, only the results normalized by leaf unit area are discussed. On the one hand due to the inverse proportionality of dry leaf weight and leaf unit area between sun-exposed and shaded leaves (Huang *et al.*, 2019), which generally results in a significantly lower dry weight of shaded over sun-exposed leaves. This manifests itself especially towards the late end of the growing season, when compounds containing sugars and nitrogen are transported from leaves into stems and roots (Dickson, 1989; Koike, 1990; Prasad and Gülz, 1990). On the other hand, sun-exposed leaves contain a larger amount of soluble sugars which additionally contribute to a larger dry leaf weight compared to shaded leaves (Castrillo *et al.*, 2005).

All investigated samples of sun-exposed leaves showed a significantly larger epicuticular wax content per leaf unit area in comparison to shaded leaves, reflecting structural differences between sun-exposed and shaded leaves in leaf thickness, leaf area (Mueller *et al.*, 2012) and carbon and nitrogen concentration (Sariyildiz and Anderson, 2003; White and Montes-R., 2005; Lichtenthaler *et al.*,2007). The observed difference in leaf properties with typically smaller and thicker sun-exposed leaves and larger but thinner shaded leaves (Figures 5 and 6) is in line with previous studies reporting structural differences in leaves of sun-exposed and shaded canopy positions within the same tree (Weraduwage *et al.*, 2015; Bender *et al.*, 2017). These differences reflect acclimation strategies that ensure the survival of the plant in high sunlight environments where transpiration and overheating often have damaging effects (Smith *et al.*, 1997; Kidner *et al.*, 2010).

The larger leaf thickness of sun-exposed leaves is related to an increased mesophyll thickness (McMillen and McClendon, 1983) that ensures a higher rate of photosynthesis per leaf unit area (Terashima *et al.*, 2001). In addition, sun-exposed leaves develop an additional layer of palisade cells as well as longer palisade cells relative to shaded leaves (Klich, 2000; Evans and Poorter, 2001; Sariyildiz and Anderson, 2003 ; Lichtenthaler *et al.*, 2007). Aside from the higher photosynthetic rate per leaf unit area in sun-exposed leaves (Terashima *et al.*, 2001), shaded leaves had a larger chlorophyll content which results in a more efficient sunlight interception (White and Montes-R., 2005). This in turn explains the slightly higher SPAD values of shaded leaves as opposed to sun-exposed leaves (Figure 4). Nevertheless, other factors like the different leaf development stage as well as the non-uniform distribution of chlorophyll over the leaf surface (Uddling *et al.*, 2007) should also be considered when interpreting SPAD values.

The generally higher photosynthetic activity in sun-exposed leaves likely results in a greater rate of carbon assimilation and thus in a greater total carbon concentration than in shaded leaves (Figure 8; Herrick and Thomas, 1999). Additionally, an increased carbon assimilation often involves an increased nitrogen assimilation (Figure 9; Nijs *et al.*, 1995). This corresponds with the results in

this study of a higher carbon and nitrogen concentration per leaf unit area in sun-exposed leaves compared to shaded leaves. This further supports the findings of Evans and Poorter (2001), who found a nitrogen concentration per leaf unit area half as high in shaded than in sun-exposed leaves. This further indicates an active modulation of leaf area as a function of sun-exposure. Consequently, under shaded conditions leaves produce a larger leaf area including a larger chlorophyll content as opposed to leaves from sun-exposed canopy positions (Perrin *et al.*, 2013). Furthermore, the increased C:N ratio from shaded to sun-exposed leaves (Figure 10) has also been observed in a study by Sariyildiz and Anderson (2003), where structural differences in sun-exposed and shaded leaves of three deciduous tree species (10 - 15 years old); sweet chestnut (*Castanea sativa* Mill), oak (*Quercus robur* L) and beech (*Fagus sylvatica* L.) were analysed. They reported a clearly increasing C:N ratio from shaded to sun-exposed leaves in all three tree species which could probably be explained by the higher concentration of sugar constituents and compounds containing nitrogen (Le Roux *et al.*, 2001; Sariyildiz and Anderson 2003). The lower water content in sun-exposed leaves (Figure 7) is in accordance with other studies, reporting a significantly lower water content in sun-exposed leaves (42%) than in shaded leaves (53%) of mature beech trees (Pilegaard *et al.*, 2003). Moreover, water content positively correlates with leaf surface area and thus results in smaller sun-exposed leaves with a lower water content (Šesták *et al.*, 1978; Lichtenthaler *et al.*, 2007).

To avoid uncontrolled water loss through evaporation, sun-exposed leaves evolved different strategies like a reduced leaf size (Kidner *et al.*, 2010) or the formation of an epicuticular wax layer (Jefferson *et al.*, 1989; Cameron *et al.*, 2006; Shepherd and Griffiths, 2006). As a result, sun-exposed leaves are characterized by a smaller leaf area with a larger epicuticular wax content than shaded leaves (Figure 12). Therefore, the ability of plants to survive in high sunlight environments depends on their capacity to reduce water loss and irradiation that enters the leaf (Huggins *et al.*, 2018). Epicuticular wax offers a protective barrier against environmental stress, including high irradiation and temperature (Shepherd and Griffiths, 2006; Huggins *et al.*, 2018), since epicuticular wax can minimize moisture loss through evapotranspiration (Holmes and Keiller, 2002; Wang *et al.*, 2019). Previous studies highlighted an increased epicuticular wax content in response to increased temperatures (Giese, 1975; Skoss, 1955; Shepherd and Griffiths, 2006; Huggins *et al.*, 2018) and increased irradiation (Steinmüller and Tevini, 1985; Kosma *et al.*, 2009). This is in line with a study by Giese (1975), who reported a 2.5 to 7.5 times thicker leaf cuticle in barley leaves grown under light exposure than in leaves grown under low light conditions. Consequently, a larger epicuticular wax amount constitutes selective advantage in high sunlight habitats (Gordon *et al.*, 1998). Furthermore, Huggins *et al.* (2018) observed an increased wax content in wheat cultures under high temperature conditions than under controlled conditions. In contrast, Baker (1974) observed a decreased epicuticular wax content with increasing temperatures (> 35 °C) and an increased epicuticular wax content at temperature of about 20 °C. Similar results were reported by Skoss (1955), who observed an increased epicuticular wax deposition at a temperature of about 17°C. Hence, the quantity of epicuticular wax formed is not only genetically but also environmentally regulated (Huggins *et al.*, 2018), particularly

by increased temperatures, irradiation (Holmes and Keiller, 2002) and water deficiency (Shepherd and Griffiths, 2006). Whether increased temperatures or increased irradiation has a greater effect on epicuticular wax formation is a question yet to be addressed, although Steinmüller and Tevini (1985) found an increased epicuticular wax formation with increasing alpine altitude caused by enhanced UV radiation.

Consequently, the rapid increase in epicuticular wax content in early August (DOY 222-228) particularly in sun-exposed leaves, could be explained by the increased solar radiation (299 W m^{-2}) and temperature (Figure 22).

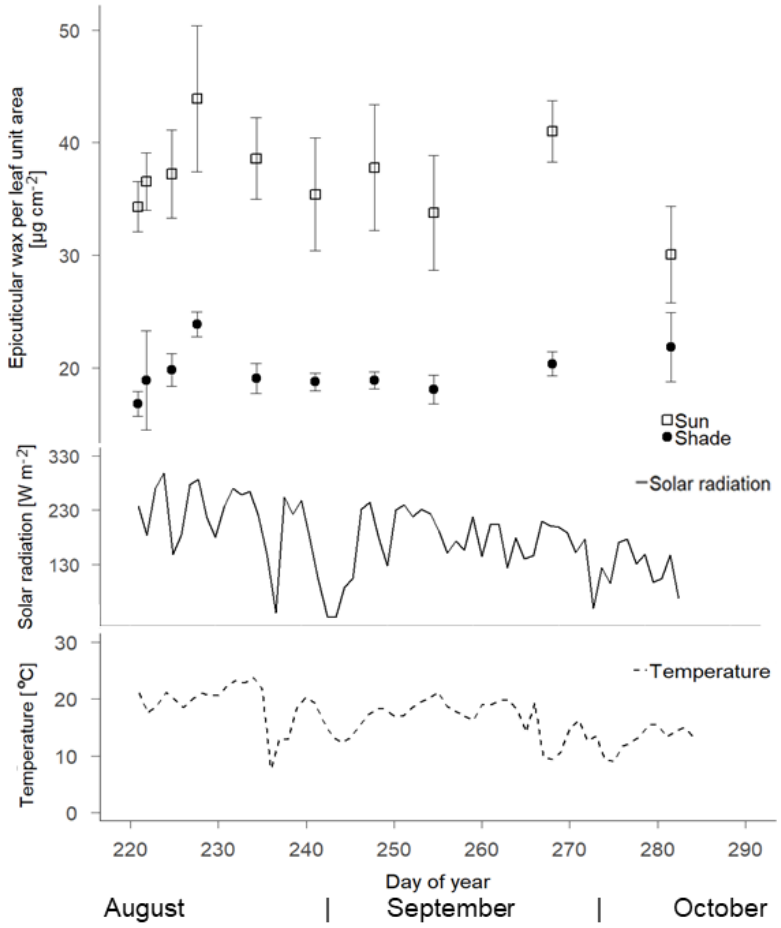

Figure 22: Epicuticular wax content of sun-exposed and shaded leaves in relation to solar radiation and sun exposure throughout the late growing season (Aug - Oct, 2018; MeteoSwiss; https://gate.meteoswiss.ch/obs, measuring station: Fluntern).

Moreover, the second increase in epicuticular wax content in late September (DOY 270) positively correlates with an increase in temperature and irradiation. The reduction of epicuticular wax content in sun-exposed leaves towards end of growing season (DOY 284) can be explained either by a

progressive wax degradation due to leaf senescence (Nguyen-Tu *et al.*, 2001) or by an overall reduction in wax synthesis (Sachse *et al.*, 2015). In contrast, shaded leaves showed an increasing trend in the epicuticular wax content as the growing season proceeded. This can be due to leaf fall starting from the outermost parts of the crown, resulting in the exposure of shaded leaves to sunlight conditions. As reported by Giese (1975), leaves grown previously under light deficiency exhibited the same amount of epictuicular wax after being exposed to light conditions for 24 hours.

4.1.1 *n*-Alkane composition

The greater *n*-alkane quantity per leaf unit area in sun-exposed than in shaded leaves, particularly in early August (Figure 14) is in line with the findings by Shepherd and Griffiths (2006), who reported an increased *n*-alkane quantity in response to increased temperatures and irradiation. Moreover, the larger *n*-alkane content in sun-exposed leaves correlates positively with water deficiency (Figure 7). Similar results were reported by Kosma *et al.* (2009), who reported a significant increase in the *n*-alkane content in Arabidopsis leaves caused by water stress. Variability in temperatures are responsible for 27% to 29% of the alteration in the average chain length of *n*-alkanes with a positive correlation between *n*-alkane chain length and increased temperature (Tipple and Pagani, 2013). Similar results were reported in other studies, where longer *n*-alkane chain lengths positively correlate with increased temperatures, due to the well-known relationship between the boiling point and number of carbon atoms (Gagosian and Peltzer, 1986; Feakins *et al.*, 2016). This, however, contradicts the findings within this study of longer n-alkane chain lengths in shaded than in sun-exposed leaves (Figures 16a and 17a) but supports the findings of Srivastava and Wiesenberg (2018), who found an increased and faster n-alkane synthesis caused by environmental stress that results in a reduced chain-elongation.

In contrast to the study of Tipple and Pagani (2013), where variability in wax composition seems to be mainly temperature regulated, Osborn and Taylor (1990) found that variability in the wax composition is dependant on light quantity. Differences in the *n*-alkane content between sun-exposed and shaded canopy position within the same tree are thus regulated by micro-climatic factors, e.g. temperature, sunlight exposition and water availability (Prasad and Gülz, 1990; Chikaraishi *et al.*, 2004; Shepherd and Griffiths, 2006; van Wittenberghe *et al.*, 2012; Bernhard and Joubès, 2013; Bush and McInerney, 2013; Tipple and Pagani, 2013). Hence, the absence of environmental stress in shaded leaves supports the results in this study of shorter *n*-alkane chain lengths in sun-exposed over shaded leaves (Figures 16a and 17b). Nevertheless, all investigated leaf samples showed a clear odd-over-even predominance with C_{27} (90%) as the dominant alkane in both sun-exposed and shaded leaves (Supplementary Figure II). This corresponds with results in the literature with C_{27} as the dominant chain length followed by followed by C_{25} (6%) and C_{29} (4%) (Gülz *et al.*, 1989; Lockheart *et al.*, 1997; Marseille *et al.*, 1999; Nguyen-Tu *et al.*, 2007; Sachse *et al.*, 2009; Piasentier *et al.*, 2000; Bush and McInerney, 2013).

4.1.2 δ^{13}C values

The range of the δ^{13}C values of bulk tissue (-29 to -30 ‰; Figure 18) and *n*-alkanes (-30 to -34 ‰; Figure 19) are in range with those for beech leaves reported by Lockheart *et al.* (1997). The observed ^{13}C depletion in shaded leaves compared to sun-exposed leaves could be explained by a higher stomatal conductance, which in turn results in a higher photosynthetic rate and more ^{13}C-depleted photosynthetic products (Waring and Silvester, 1994). This higher photosynthetic capacity is achieved because the stomata of shaded leaves mostly remain open during the day due to the absence of direct sunlight exposure and lower temperatures (Giese 1975; Stuiver and Braziunas, 1987; Damesin *et al.*, 1998) which does not affect the sun-exposed leaves. Therefore, direct sunlight exposure and increased temperatures result in stomata closure and in more ^{13}C-enriched photosynthetic products (Waring and Silvester, 1994; Feller and Vaseva, 2014). Consequently, the ^{13}C-enrichment in sun-exposed leaves can be explained by increased temperatures inside the labelling chambers of more than 30 °C and thus a higher evapotranspiration, which result in partial stomata closure and consequently a reduced photosynthetic capacity (Feller and Vaseva, 2014).

Leaves within the same tree and even on the same branch have a different stomatal conductance due to differences in sun exposure and water availability, which results in a high variability in δ^{13}C values (Waring and Silvester, 1994). However, the identical δ^{13}C values of leaves from the topmost and the terminal part of the same branch in this study (Supplementary Figures III a and b) contradict the findings of Waring and Silvester (1994), who reported a larger depletion in δ^{13}C values in leaves of the topmost part compared to leaves of the terminal part of the same branch. These differences are mainly caused by differences in sun exposure, as leaves of the terminal part of the branch are more exposed to direct sunlight than leaves from the topmost part of the branch. Thus, the equal δ^{13}C values of leaves from the topmost and the terminal parts of the same branch reported in this study could be explained by the fact that the selected branches were much shorter (0.5-0.7m) compared to the branches (0.5-10m) analysed by Waring and Silvester (1994). The leaves analysed in this study were on branches that were either completely shaded or completely sun-exposed (Supplementary Figures I a and b), which minimizes the difference in photosynthetic capacity and stomatal conductance between leaves of the same branch.

The observed ^{13}C depletion of 3‰ in *n*-alkanes compared to bulk tissue (Figures 20 and 21) is in good agreement with results of other studies, that reported a ^{13}C depletion in lipids of 2 and 9‰ of epicuticular waxes of numerous plant species relative to bulk tissue (Collister *et al.*, 1994; Ballentine *et al.*, 1998; Schleser, 1990; Conte *et al.*, 2003). This depletion can be explained by the fact that a larger amount of the assimilated ^{13}C is required for leaf sugars (Gessler *et al.*, 2001), whereof only a minor amount of assimilated ^{13}C is used for lipid synthesis (Desalme *et al.*, 2017) and by isotope fractionation during the oxidation of pyruvate to coenzyme-A in lipid biosynthesis (De Niro and Epstein, 1977; Collister *et al.*, 1994). However, the numerous funghi and bacteria that colonize leaf surfaces should not be neglected and may contribute to higher ^{13}C values in bulk tissue compared to *n*-alkanes (Collister *et al.*, 1994). In addition, the observed time lag in ^{13}C assimilation between lipids

and bulk tissue reflects both the time required to fill the precursor pool and the increased distance of required products from the labelling source (Allen *et al.*, 2015).

4.2 Renewal rate of epicuticular waxes

The overall faster wax renewal rate in sun-exposed compared to shaded leaves further supports the theory that wax biosynthesis is regulated by environmental stress such as sun exposure (Barnes *et al.*, 1996), increased temperatures (Tipple and Pagani, 2013) and water availability (Shepherd and Griffiths, 2006; Kosma *et al.*, 2009). Similar results were observed by Rentschler (1971) and by Mortazavi *et al.* (2009), who observed remarkably fast wax renewal between a few hours and days in young and mature leaves of pine trees driven by exposition to environmental stress. A faster wax renewal rate is thus of great importance to ensure a plant's growth and survival as removal of epicuticular waxes results in reduced reflectance (Holmes and Keiller, 2002) and transpiration rates (Huggins *et al.*, 2018).

The overall enrichment in ^{13}C in *n*-alkanes of both sun-exposed and shaded leaves indicates an active replacement of epicuticular waxes (Figures 19 and 21; Gao *et al.*, 2012). Other indicators such as the variability in the *n*-alkane quantity and average chain length, also support the notion of an ongoing wax formation (Neinhuis *et al.*, 2001; Tipple *et al.*, 2013). The results found within this study of a relatively stable average chain length, particularly in sun-exposed leaves, contradict with these results suggesting the absence of an active epicuticular wax formation. Nevertheless, according to Huang *et al.* (2018), a relatively constant average chain length is not an indicator of a missing epicuticular wax formation. It is rather an indicator of an active epicuticular wax formation that represents the balance between wax removal and renewal without modifying its molecular structure.

5 Conclusion

Cuticular waxes form a natural barrier between the plant's surface and its external environment, with protection against solar radiation and uncontrolled water loss as its main function. Through exposure to sunlight or increased temperatures leaves form an outermost wax layer, know as epicuticular wax, to protect the leaf against UV damage. Moreover, the quantity and composition of the epicuticular wax is genetically and environmentally regulated. This results in different epicuticular wax quantities and compositions in leaves within the same plant. Particularly leaves in sun-exposed canopy positions have a larger epicuticular wax quantity compared to shaded leaves. Consequently, solar irradiation causes an increase in the total epicuticular wax content, including *n*-alkanes. On the other hand, the variability in the wax composition, particularly in the average chain length is mainly regulated by both sun-exposure and temperature.

In this study, the quantity, composition and renewal rate of epicuticular wax was investigated in a mature beech tree throughout the late growing season (Aug - Oct, 2018). A larger epicuticular wax content and *n*-alkane content per leaf unit area was found in sun-exposed than in shaded leaves. Moreover, the wax renewal rate in sun-exposed leaves was 27 times faster than in shaded leaves. Consequently, quantity and renewal rate of epicuticuar wax depends on environmental variables such as sun exposure, temperatures and water availability.

6 Implications and Limitations

$\delta^{13}C$ isotope composition

The use of $\delta^{13}C$ values as a molecular proxy provides insights into the carbon-plant allocation and thus contributes to an improved understanding of a plant's response to environmental induced stress (Conte *et al.*, 2003). However, this environmental dependance can lead to difficulties in the interpretation of $\delta^{13}C$ values since the variability in water availability and temperature over the duration of a growing season results in different ^{13}C values within a plant (Zimmerman and Ehleringer, 1990; Dawson *et al.*, 2002). Moreover, there is a difference in the ^{13}C values between spring and autumn leaves, since autumn leaves are more depleted in ^{13}C than spring leaves (Lockheart *et al*, 1997). Therefore, additional experiments in different stage of the growing season would contribute to a better understanding of isotopic composition as well as leaf water and carbon fluxes.

n-Alkane composition

n-Alkanes are often used as a molecular proxy in soils to reconstruct climate induced changes in the geological past (Bender *et al.*, 2017). Understanding the *n*-alkane content in leaves of trees thus contributes to a better understanding about how biomarkers extracted from soils where built and the climate conditions at that time. Nevertheless, the quantity and composition of *n*-alkanes varies with the exposure to environmental stress (Shepherd and Griffiths, 2006; Bush and McInerney, 2013). This results in a large variability in the quantity and composition of *n*-alkanes in leaves within the same tree. Specifically, the average chain length reacts sensitively to environmental stress, e.g. sun exposure, increased temperature and water deficiency (Osborn and Taylor, 1990; Tipple and Pagani, 2013). In this study, *n*-alkane modification was analysed in the late end of one growing season. In order to understand the effect of environmental stress on *n*-alkane quantity and composition, the effects should be analysed over several growing seasons. Moreover, as the respective proportion of *n*-alkanes varies from leaf to leaf and leaf age, additional wax constituents should be analysed to ensure a clear identification of the quantity of newly formed waxes. Therefore, additional studies on different plant types, on identical plant types of a different age as well as in different ecosystems can improve the knowledge about leaf wax formation.

7 Outlook

Further research is needed in the identification of the wax renewal rate, specifically between young and mature trees. This contributes to an improved knowledge of a plant's metabolism and growth, which further improves the knowledge about wax formation in dependance of its abiotic and biotic environment. Furthermore, detailed information on interactions and individual effects of these factors contribute to an improved understanding of a plant's response to high sunlight and temperature environments. This will become increasingly important in the upcoming century, especially for European forest (e.g beech trees), with regard to the development of strategies that enable forest stands to withstand increased temperatures, low precipitation regimes and high irradiation levels.

References

Abràmoff, M. D., Magalhães, P. J., and Ram, S. J. (2004). Image processing with ImageJ. *Biophotonics International*, 11, 36-42.

Allen, D. K., Bates, P. D., and Tjellstroem, H. (2015). Tracking the metabolic pulse of plant lipid production with isotopic labelling and flux analyses: Past, present and future. *Progress in Lipid Research*, 58, 97-120.

Ardenghi, N., Mulch, A., Pross, J., and Niedermeyer, E. M. (2017). Leaf wax *n*-alkane extraction: An optimised procedure. *Organic Geochemistry*, 113, 283-292.

Bahn, M., Lattanzi, F. A., Hasibeder, R., Wild, B., Koranda, M., Danese, V., Brüggemann, N., Schmitt, M., Siegwolf, R., and Richter, A. (2013). Responses of belowground carbon allocation dynamics to extended shading in mountain grassland. *New Phytologist*, 198, 116-126.

Baker, E. A. (1974). The influence of environment on leaf wax development in *Brassica oleracea* var. *gemmifera*. *New Phytologist*, 73, 955-966.

Ballentine, D. C., Macko, S. A., and Turekian, V. C. (1998). Variability of stable carbon isotopic compositions in individual fatty acids from combustion of C_4 and C_3plants: Implications for biomass burning. *Chemical Geology*, 152, 151-161.

Bargel, H., Koch, K., Cerman, Z., and Neinhuis, C. (2006). Evans Review No. 3: Structure-function relationships of the plant cuticle and cuticular waxes-a smart material? *Functional Plant Biology*, 33, 893-910.

Barnes, J. D., Percy, K. E., Paul, N. D., Jones, P., McLaughlin, C. K., Mullineaux, P. M., Creissen, G. and Wellburn, A. R. (1996). The influence of UV-B radiation on the physicochemical nature of tobacco (*Nicotiana tabacum* L.) leaf surfaces. *Journal of Experimental Botany*, 47, 99-109.

Bender, A. L., Chitwood, D. H., and Bradley, A. S. (2017). Heritability of the structures and ^{13}C fractionation in tomato leaf wax alkanes: A genetic model system to inform paleoenvironmental reconstructions. *Frontiers in Earth Science*, 5, 47.

Bernard, A., and Joubès, J. (2013). Arabidopsis cuticular waxes: Advances in synthesis, export and regulation. *Progress in Lipid Research*, 52, 110-129.

Blessing, C. H., Werner, R. A., Siegwolf, R., and Buchmann, N. (2015). Allocation dynamics of recently fixed carbon in beech saplings in response to increased temperatures and drought. *Tree Physiology*, 35, 585-598.

Buschhaus, C., Herz, H., and Jetter, R. (2007). Chemical composition of the epicuticular and intracuticular wax layers on the adaxial side of *Ligustrum vulgare* leaves. *New Phytologist*, 176, 311-316.

Bush, R. T., and McInerney, F. A. (2013). Leaf wax *n*-alkane distributions in and across modern plants: Implications for paleoecology and chemotaxonomy. *Geochimica et Cosmochimica Acta*, 117, 161-179.

Cameron, K. D., Teece, M. A., and Smart, L. B. (2006). Increased accumulation of cuticular wax and expression of lipid transfer protein in response to periodic drying events in leaves of tree tobacco. *Plant Physiology*, 140, 176-183.

Castrillo, M., Vizcaíno, D., Moreno, E., and Latorraca, Z. (2005). Specific leaf mass, fresh: Dry weight ratio, sugar and protein contents in species of *Lamiaceae* from different light environments. *Revista de Biologia Tropical*, 53, 23-28.

Chikaraishi, Y., Naraoka, H., and Poulson, S. R. (2004). Carbon and hydrogen isotopic fractionation during lipid biosynthesis in a higher plant (*Cryptomeria japonica*). *Phytochemistry*, 65, 323-330.

Collister, J. W., Rieley, G., Stern, B., Eglinton, G., and Fry, B. (1994). Compound-specific δ^{13}C analyses of leaf lipids from plants with differing carbon dioxide metabolisms. *Organic Geochemistry*, 21, 619-627.

Conte, M. H., Weber, J. C., Carlson, P. J., and Flanagan, L. B. (2003). Molecular and carbon isotopic composition of leaf wax in vegetation and aerosols in a northern prairie ecosystem. *Oecologia*, 135, 67-77.

Damesin, C., Rambal, S., and Joffre, R. (1998). Seasonal and annual changes in leaf δ^{13}C in two co-occurring Mediterranean oaks: relations to leaf growth and drought progression. *Functional Ecology*, 12, 778-785.

Dawson, T. E., Mambelli, S., Plamboeck, A. H., Templer, P. H., and Tu, K. P. (2002). Stable isotopes in plant ecology. *Annual Review of Ecology and Systematics*, 33, 507-559.

DeNiro, M. J., and Epstein, S. (1977). Mechanism of carbon isotope fractionation associated with lipid synthesis. *Science*, 197, 261-263.

Desalme, D., Priault, P., Gérant, D., Dannoura, M., Maillard, P., Plain, C., and Epron, D. (2017). Seasonal variations drive short-term dynamics and partitioning of recently assimilated carbon in the foliage of adult beech and pine. *New Phytologist*, 213, 140-153.

Dickson, R. E. (1989). Carbon and nitrogen allocation in trees. *Annales des Sciences Forestières*, 46, 631-647. EDP Sciences.

Diefendorf, A. F., Freeman, K. H., Wing, S. L., and Graham, H. V. (2011). Production of *n*-alkyl lipids in living plants and implications for the geologic past. *Geochimica et Cosmochimica Acta*, 75, 7472-7485.

Diefendorf, A. F., and Freimuth, E. J. (2017). Extracting the most from terrestrial plant-derived *n*-alkyl lipids and their carbon isotopes from the sedimentary record: A review. *Organic Geochemistry*, 103, 1-21.

Dodd, R. S., and Poveda, M. M. (2003). Environmental gradients and population divergence contribute to variation in cuticular wax composition in *Juniperus communis*. *Biochemical Systematics and Ecology*, 31, 1257-1270.

Dyckmans, J., Flessa, H., Brinkmann, K., Mai, C., and Polle, A. (2002). Carbon and nitrogen dynamics in acid detergent fibre lignins of beech (*Fagus sylvatica* L.) during the growth phase. *Plant, Cell and Environment*, 25, 469-478.

Easlon, H. M., and Bloom, A. J. (2014). Easy leaf area: Automated digital image analysis for rapid and accurate measurement of leaf area. *Applications in Plant Sciences*, 2, 1-4.

Eglinton, G., and Hamilton, R. J. (1967). Leaf epicuticular waxes. *Science*, 156, 1322-1335.

Eglinton, T. I., and Eglinton, G. (2008). Molecular proxies for paleoclimatology. *Earth and Planetary Science Letters*, 275, 1-16.

England, J. R., and Attiwill, P. M. (2006). Changes in leaf morphology and anatomy with tree age and height in the broadleaved evergreen species, Eucalyptus regnans F. Muell. *Trees*, 20, 79.

Epron, D., Bahn, M., Derrien, D., Lattanzi, F. A., Pumpanen, J., Gessler, A.,Högberg, P., Maillard, P.,Dannoura, M., Gérant, D., and Buchmann, N. (2012). Pulse-labelling trees to study carbon allocation dynamics: A review of methods, current knowledge and future prospects. *Tree Physiology*, 32, 776-798.

Evans, J., and Poorter, H. (2001). Photosynthetic acclimation of plants to growth irradiance: The relative importance of specific leaf area and nitrogen partitioning in maximizing carbon gain. *Plant, Cell and Environment*, 24, 755-767.

Feakins, S. J., Peters, T., Wu, M. S., Shenkin, A., Salinas, N., Girardin, C. A., Bentley, L.P., Blonder, B., Enquist, B.J., Asner, G. P. and Malhi, Y. (2016). Production of leaf wax *n*-alkanes across a tropical forest elevation transect. *Organic Geochemistry*, 100, 89-100.

Feller, U., and Vaseva, I. I. (2014). Extreme climatic events: Impacts of drought and high temperature on physiological processes in agronomically important plants. *Frontiers in Environmental Science*, 2, 39.

Gagosian, R. B., and Peltzer, E. T. (1986). The importance of atmospheric input of terrestrial organic material to deep sea sediments. *Organic Geochemistry*, 10, 661-669.

Gao, L., Burnier, A., and Huang, Y. (2012). Quantifying instantaneous regeneration rates of plant leaf waxes using stable hydrogen isotope labeling. *Rapid Communications in Mass Spectrometry*, 26, 115-122.

Gessler, A., Schrempp, S., Matzarakis, A., Mayer, H., Rennenberg, H., and Adams, M. A. (2001). Radiation modifies the effect of water availability on the carbon isotope composition of beech (*Fagus sylvatica*). *New Phytologist*, 150, 653-664.

Giese, B. N. (1975). Effects of light and temperature on the composition of epicuticular wax of barley leaves. *Phytochemistry*, 14, 921-929.

Gordon, D. C., Percy, K. E., and Riding, R. T. (1998). Effects of UV-B radiation on epicuticular wax production and chemical composition of four *Picea* species. *The New Phytologist*, 138, 441-449.

Gülz, P. G., Müller, E., and Prasad, R. B. N. (1989). Organ-specific composition of epicuticular waxes of beech (*Fagus sylvatica* L.) leaves and seeds. *Zeitschrift für Naturforschung C*, 44, 731-734.

Hauke, V., and Schreiber, L. (1998). Ontogenetic and seasonal development of wax composition and cuticular transpiration of ivy (*Hedera helix* L.) sun and shade leaves. *Planta*, 207, 67-75.

Herrick, J. D., and Thomas, R. B. (1999). Effects of CO_2 enrichment on the photosynthetic light response of sun and shade leaves of canopy sweetgum trees (*Liquidambar styraciflua*) in a forest ecosystem. *Tree Physiology*, 19, 779-786.

Heinrich, S., Dippold, M. A., Werner, C., Wiesenberg, G. L., Kuzyakov, Y., and Glaser, B. (2015). Allocation of freshly assimilated carbon into primary and secondary metabolites after in situ ^{13}C pulse labelling of Norway spruce (*Picea abies*). *Tree Physiology*, 35, 1176-1191.

Hoffmann, B., Kahmen, A., Cernusak, L. A., Arndt, S. K., and Sachse, D. (2013). Abundance and distribution of leaf wax *n*-alkanes in leaves of Acacia and Eucalyptus trees along a strong humidity gradient in northern Australia. *Organic Geochemistry*, 62, 62-67.

Holmes, M. G., and Keiller, D. R. (2002). Effects of pubescence and waxes on the reflectance of leaves in the ultraviolet and photosynthetic wavebands: A comparison of a range of species. *Plant, Cell and Environment*, 25, 85-93.

Huang, X., Zhao, B., Wang, K., Hu, Y., and Meyers, P. A. (2018). Seasonal variations of leaf wax *n*-alkane molecular composition and δD values in two subtropical deciduous tree species: Results from a three-year monitoring program in central China. *Organic Geochemistry*, 118, 15-26.

Huang, W., Ratkowsky, D. A., Hui, C., Wang, P., Su, J., and Shi, P. (2019). Leaf fresh weight versus dry weight: Which is better for describing the scaling relationship between leaf biomass and leaf area for broad-leaved plants? *Forests*, 10, 256.

Huggins, T. D., Mohammed, S., Sengodon, P., Ibrahim, A. M. H., Tilley, M., and Hays, D. B. (2018). Changes in leaf epicuticular wax load and its effect on leaf temperature and physiological traits in wheat cultivars (*Triticum aestivum* L.) exposed to high temperatures during anthesis. *Journal of Agronomy and Crop Science*, 204, 49-61.

Jansen, B., and Wiesenberg, G. L. (2017). Opportunities and limitations related to the application of plant-derived lipid molecular proxies in soil science. *Soil*, 3, 211-234.

Jefferson, P. G., Johnson, D. A., Rumbaugh, M. D., and Asay, K. H. (1989). Water stress and genotypic effects on epicuticular wax production of alfalfa and crested wheatgrass in relation to yield and excised leaf water loss rate. *Canadian Journal of Plant Science*, 69, 481-490.

Jetter, R., Schäffer, S., and Riederer, M. (2000). Leaf cuticular waxes are arranged in chemically and mechanically distinct layers: Evidence from *Prunus laurocerasus* L. *Plant, Cell and Environment*, 23, 619-628.

Jetter, R., and Schäffer, S. (2001). Chemical composition of the *Prunus laurocerasus* leaf surface. Dynamic changes of the epicuticular wax film during leaf development. *Plant Physiology*, 126, 1725-1737.

Jetter, R., and Kunst, L. (2008). Plant surface lipid biosynthetic pathways and their utility for metabolic engineering of waxes and hydrocarbon biofuels. *The Plant Journal*, 54, 670-683.

Kagawa, A., Sugimoto, A., Yamashita, K., and Abe, H. (2005). Temporal photosynthetic carbon isotope signatures revealed in a tree ring through $^{13}CO_2$ pulse-labelling. *Plant, Cell and Environment*, 28, 906-915.

Kidner, C. A., and Umbreen, S. (2010). Why is leaf shape so variable. *International Journal of Plant Developmental Biology*, 4, 64-75.

Klich, M. G. (2000). Leaf variations in *Elaeagnus angustifolia* related to environmental heterogeneity. *Environmental and Experimental Botany*, 44, 171-183.

Knight, T. G., Wallwork, M. A., and Sedgley, M. (2004). Leaf epicuticular wax and cuticle ultrastructure of four Eucalyptus species and their hybrids. *International Journal of Plant Sciences*, 165, 27-36.

Koch, K., Bhushan, B., and Barthlott, W. (2009). Multifunctional surface structures of plants: An inspiration for biomimetics. *Progress in Materials Science*, 54, 137-178.

Koike, T. (1990). Autumn coloring, photosynthetic performance and leaf development of deciduous broad-leaved trees in relation to forest succession. *Tree Physiology*, 7, 21-32.

Kolattukudy, P. E., and Walton, T. J. (1973). The biochemistry of plant cuticular lipids. *Progress in the Chemistry of Fats and other Lipids*, 13, 119-175.

Kosma, D. K., Bourdenx, B., Bernard, A., Parsons, E. P., Lü, S., Joubès, J., and Jenks, M. A. (2009). The impact of water deficiency on leaf cuticle lipids of Arabidopsis. *Plant Physiology*, 151, 1918-1929.

Kunst, L., and Samuels, A. L. (2003). Biosynthesis and secretion of plant cuticular wax. *Progress in Lipid Research*, 42, 51-80.

Lacointe, A., Deleens, E., Ameglio, T., Saint-Joanis, B., Lelarge, C., Vandame, M., Song, G.C., and Daudet, F. A. (2004). Testing the branch autonomy theory: A $^{13}C/^{14}C$ double-labelling experiment on differentially shaded branches. *Plant, Cell and Environment*, 27, 1159-1168.

Laila, R., Robin, A. H. K., Yang, K., Park, J. I., Suh, M. C., Kim, J., and Nou, I. S. (2017). Developmental and genotypic variation in leaf wax content and composition, and in expression of wax biosynthetic genes in *Brassica oleracea* var.*capitata*. *Frontiers in Plant Science*, 7, 1972.

Le Roux, X., Walcroft, A. S., Daudet, F. A., Sinoquet, H., Chaves, M. M., Rodrigues, A., and Osorio, L. (2001). Photosynthetic light acclimation in peach leaves: Importance of changes in mass: Area ratio, nitrogen concentration, and leaf nitrogen partitioning. *Tree Physiology*, 21, 377-386.

Li, R., Meyers, P. A., Fan, J., and Xue, J. (2016). Monthly changes in chain length distributions and stable carbon isotope composition of leaf *n*-alkanes during growth of the bamboo *Dendrocalamus ronganensis* and the grass *Setaria viridis*. *Organic Geochemistry*, 101, 72-81.

Li, X., Anderson, B. J., Vogeler, I., and Schwendenmann, L. (2018). Long-chain *n*-alkane and *n*-fatty acid characteristics in plants and soil-potential to separate plant growth forms, primary and secondary grasslands? *Science of the Total Environment*, 645, 1567-1578.

Lichtenthaler, H. K., Ač, A., Marek, M. V., Kalina, J., and Urban, O. (2007). Differences in pigment composition, photosynthetic rates and chlorophyll fluorescence images of sun and shade leaves of four tree species. *Plant Physiology and Biochemistry*, 45, 577-588.

Lockheart, M. J., Van Bergen, P. F., and Evershed, R. P. (1997). Variations in the stable carbon isotope compositions of individual lipids from the leaves of modern angiosperms: Implications for the study of higher land plant-derived sedimentary organic matter. *Organic Geochemistry*, 26, 137-153.

Marseille, F., Disnar, J. R., Guillet, B., and Noack, Y. (1999). *n*-Alkanes and free fatty acids in humus and A1 horizons of soils under beech, spruce and grass in the Massif-Central (Mont-Lozère), France. *European Journal of Soil Science*, 50, 433-441.

McMillen, G. G., and McClendon, J. H. (1983). Dependence of photosynthetic rates on leaf density thickness in deciduous woody plants grown in sun and shade. *Plant Physiology*, 72, 674-678.

MeteoSwiss (2018). *http://www.meteoschweiz.admin.ch* (last accessed, 27.09.2018)

MeteoSwiss (2018). *https://gate.meteoswiss.ch/idaweb* (last accessed, 27.09.2018)

Mueller, K. E., Polissar, P. J., Oleksyn, J., and Freeman, K. H. (2012). Differentiating temperate tree species and their organs using lipid biomarkers in leaves, roots and soil. *Organic Geochemistry*, 52, 130-141.

Müller, C., and Riederer, M. (2005). Plant surface properties in chemical ecology. *Journal of Chemical Ecology*, 31, 2621-2651.

Mortazavi, B., Conte, M. H., Chanton, J. P., Smith, M. C., Weber, J. C., Crumsey, J., and Ghashghaie, J. (2009). Does the ^{13}C of foliage-respired CO_2 and biochemical pools reflect the ^{13}C of recently assimilated carbon? *Plant, Cell and Environment*, 32, 1310-1323.

Neinhuis, C., Koch, K., and Barthlott, W. (2001). Movement and regeneration of epicuticular waxes through plant cuticles. *Planta*, 213, 427-434.

Nijs, I., Behaeghe, T., and Impens, I. (1995). Leaf nitrogen content as a predictor of photosynthetic capacity in ambient and global change conditions. *Journal of Biogeography*, 177-183.

Nelson, D. B., Knohl, A., Sachse, D., Schefuss, E., and Kahmen, A. (2017). Sources and abundances of leaf waxes in aerosols in central Europe. *Geochimica et Cosmochimica Acta*, 198, 299-314.

Nguyen-Tu, T.T., Derenne, S., Largeau, C., Mariotti, A., and Bocherens, H. (2001). Evolution of the chemical composition of *Ginkgo biloba* external and internal leaf lipids through senescence and litter formation.*Organic Geochemistry*, 32, 45-55.

Nguyen-Tu, T. T., Egasse, C., Zeller, B., and Derenne, S. (2007). Chemotaxonomical investigations of fossil and extant beeches. I. Leaf lipids from the extant *Fagus sylvatica* L. *Comptes Rendus Palevol*, 6, 451-461.

Nogués, S., Damesin, C., Tcherkez, G., Maunoury, F., Cornic, G., and Ghashghaie, J. (2006). $^{13}C/^{13}C$ isotope labelling to study leaf carbon respiration and allocation in twigs of field-grown beech trees. *Rapid Communications in Mass Spectrometry: An International Journal Devoted to the Rapid Dissemination of Up-to-the-Minute Research in Mass Spectrometry*, 20, 219-226.

O'Neal, M. E., Landis, D. A., and Isaacs, R. (2002). An inexpensive, accurate method for measuring leaf area and defoliation through digital image analysis. *Journal of Economic Entomology*, 95, 1190-1194.

Osborn, J. M., and Taylor, T. N. (1990). Morphological and ultrastructural studies of plant cuticular membranes. I. Sun and shade leaves of Quercus velutina (*Fagaceae*). *Botanical Gazette*, 151, 465-476.

Pancost, R. D., and Boot, C. S. (2004). The palaeoclimatic utility of terrestrial biomarkers in marine sediments. *Marine Chemistry*, 92, 239-261.

Perrin, P. M., and Mitchell, F. J. (2013). Effects of shade on growth, biomass allocation and leaf morphology in European yew (*Taxus baccata* L.). *European Journal of Forest Research*, 132, 211-218.

Piasentier, E., Bovolenta, S., and Malossini, F. (2000). The *n*-alkane concentrations in buds and leaves of browsed broadleaf trees. *The Journal of Agricultural Science*, 135, 311-320.

Pilegaard, K., Mikkelsen, T. N., Beier, C., Jensen, N. O., Ambus, P., and Ro-Poulsen, H. (2003). Field measurements of atmosphere-biosphere interactions in a Danish beech forest. *Boreal Environment Research*, 8, 315-334.

Prasad, R. B. N., and Gülz, P. G. (1990). Developmental and Seasonal Variations in the Epicuticular Waxes of Beech Leaves (*Fagus sylvatica* L.). *Zeitschrift für Naturforschung C*, 45, 805-812.

RStudio Team (2016). RStudio: Integrated Development for R. *RStudio, Inc., Boston, MA*.

Reina-Pinto, J. J., and Yephremov, A. (2009). Surface lipids and plant defenses. *Plant Physiology and Biochemistry*, 47, 540-549.

Rentschler, I. (1971). Die Wasserbenetzbarkeit von Blattoberflächen und ihre submikroskopische Wachsstruktur. *Planta*, 96, 119-135.

Sachse, D., Kahmen, A., and Gleixner, G. (2009). Significant seasonal variation in the hydrogen isotopic composition of leaf-wax lipids for two deciduous tree ecosystems (*Fagus sylvativa* and *Acerpseudoplatanus*). *Organic Geochemistry*, 40, 732-742.

Sachse, D., Dawson, T. E., and Kahmen, A. (2015). Seasonal variation of leaf wax *n*-alkane production and δ^2H values from the evergreen oak tree, *Quercus agrifolia*. *Isotopes in Environmental and Health Studies*, 51, 124-142.

Samuels, L., Kunst, L., and Jetter, R. (2008). Sealing plant surfaces: Cuticular wax formation by epidermal cells. *Annual Review of Plant Biology.*, 59, 683-707.

Sariyildiz, T., and Anderson, J. M. (2003). Decomposition of sun and shade leaves from three deciduous tree species, as affected by their chemical composition. *Biology and Fertility of Soils*, 37, 137-146.

Schleser, G. H. (1990). Investigations of the $\delta^{13}C$ pattern in leaves of *Fagus sylvatica* L. *Journal of Experimental Botany*, 41, 565-572.

Šesták, Z., Solárová, J., Zima, J., and Václavák, J. (1978). Effect of Growth Irradiance on Photosynthesis and Transpiration in *Phaseolus vulgaris* L. *Biologia Plantarum,* 20, 234-238.

Shepherd, T., and Griffiths, D. (2006). The effects of stress on plant cuticular waxes. *New Phytologist*, 171, 469-499.

Skoss, J. D. (1955). Structure and composition of plant cuticle in relation to environmental factors and permeability. *Botanical Gazette*, 117, 55-72.

Smith, W. K., Vogelmann, T. C., DeLucia, E. H., Bell, D. T., and Shepherd, K. A. (1997). Leaf form and photosynthesis. *Bioscience*, 47, 785-793.

Srivastava, K., Jentsch, A., Kreyling, J., Glaser, B., and Wiesenberg, G. L. (2017). Short-term carbon dynamics in a temperate grassland and heathland ecosystem exposed to 104 days of drought followed by irrigation. *Isotopes in Environmental and Health Studies*, 54, 41-62.

Srivastava, K., and Wiesenberg, G. L. (2018). Severe drought-influenced composition and $\delta^{13}C$ of plant and soil *n*-alkanes in model temperate grassland and heathland ecosystems. *Organic Geochemistry*, 116, 77-89.

Stuiver, M., and Braziunas, T. F. (1987). Tree cellulose $^{13}C/^{12}C$ isotope ratios and climatic change. *Nature*, 328, 58.

Steinmüller, D., and Tevini, M. (1985). Action of ultraviolet radiation (UV-B) upon cuticular waxes in some crop plants. *Planta*, 164, 557-564.

Swisstopo. *http:// map.geo.admin.ch* (last accessed: 27.09.2018)

Terashima, I., Miyazawa, S. I., and Hanba, Y. T. (2001). Why are sun leaves thicker than shade leaves?- Consideration based on analyses of CO_2 diffusion in the leaf. *Journal of Plant Research*, 114, 93-105.

Tipple, B. J., Berke, M. A., Doman, C. E., Khachaturyan, S., and Ehleringer, J. R. (2013). Leaf-wax *n*-alkanes record the plant-water environment at leaf flush. *Proceedings of the National Academy of Sciences*, 110, 2659-2664.

Tipple, B. J., and Pagani, M. (2013). Environmental control on eastern broadleaf forest species' leaf wax distributions and D/H ratios. *Geochimica et Cosmochimica Acta*, 111, 64-77.

Uddling, J., Gelang-Alfredsson, J., Piikki, K., and Pleijel, H. (2007). Evaluating the relationship between leaf chlorophyll concentration and SPAD-502 chlorophyll meter readings. *Photosynthesis Research*, 91, 37-46.

van Maarseveen, C., and Jetter, R. (2009). Composition of the epicuticular and intracuticular wax layers on *Kalanchoe daigremontiana* (Hamet et Perr. de la Bathie) leaves. *Phytochemistry*,70, 899-906.

van Wittenberghe, S., Adriaenssens, S., Staelens, J., Verheyen, K., and Samson, R. (2012). Variability of stomatal conductance, leaf anatomy, and seasonal leaf wettability of young and adult European beech leaves along a vertical canopy gradient. *Trees*, 26, 1427-1438.

Vitousek, P. M., Field, C. B., and Matson, P. A. (1990). Variation in foliar $\delta^{13}C$ in Hawaiian *Metrosideros polymorpha*: a case of internal resistance? *Oecologia*, 84, 362-370.

Vogts, A., Moossen, H., Rommerskirchen, F., and Rullkötter, J. (2009). Distribution patterns and stable carbon isotopic composition of alkanes and alkan-1-ols from plant waxes of African rain forest and savanna C_3 species. *Organic Geochemistry*, 40, 1037-1054.

Wang, C., He, J., Zhao, T. H., Cao, Y., Wang, G., Sun, B., Yan, X., Guo, W., and Li, M. H. (2019). The smaller the leaf is, the faster the leaf water loses in a temperate forest. *Frontiers in Plant Science*, 10, 58.

Waring, R. H., and Silvester, W. B. (1994). Variation in foliar $\delta^{13}C$ values within the crowns of *Pinus radiata* trees. *Tree Physiology*, 14, 1203-1213.

Weraduwage, S. M., Chen, J., Anozie, F. C., Morales, A., Weise, S. E., and Sharkey, T. D. (2015). The relationship between leaf area growth and biomass accumulation in Arabidopsis thaliana. *Frontiers in Plant Science*, 6, 167.

White, J. W., and Montes-R., C. (2005). Variation in parameters related to leaf thickness in common bean (*Phaseolus vulgaris* L.). *Field Crops Research*, 91, 7-21.

Wiesenberg, G. L., Schwarzbauer, J., Schmidt, M. W., and Schwark, L. (2004). Source and turnover of organic matter in agricultural soils derived from *n*-alkane/*n*-carboxylic acid compositions and C-isotope signatures. *Organic Geochemistry*, 35, 1371-1393.

Wiesenberg, G. L., Schneckenberger, K., Kuzyakov, Y., and Schwark, L. (2009). Plant lipid composition is not affected by short-term isotopic (^{13}C) pulse-labelling experiments. *Journal of Plant Nutrition and Soil Science*, 172, 445-453.

Wiesenberg, G.L.B., and Gocke, M.I., (2017). Analysis of Lipids and Polycyclic Aromatic Hydrocarbons as Indicators of Past and Present (Micro-)Biological Activity, in: McGenity, T.J., N., T.K., Nogales Fernández, B. (Eds.), *Hydrocarbon and Lipid Microbiology Protocols - Petroleum, Hydrocarbon and Lipid Analysis.* Springer, Berlin, Heidelberg, 61-91.

Zhang, H. Y., Hartmann, H., Gleixner, G., Thoma, M., and Schwab, V. F. (2019). Carbon isotope fractionation including photosynthetic and post-photosynthetic processes in C_3 plants: Low [CO_2] matters. *Geochimica et Cosmochimica Acta*, 245, 1-15.

Zimmerman, J. K., and Ehleringer, J. R. (1990). Carbon isotope ratios are correlated with irradiance levels in the Panamanian orchid *Catasetum viridiflavum*. *Oecologia*, 83, 247-249.

Appendix

(a) Shaded canopy position

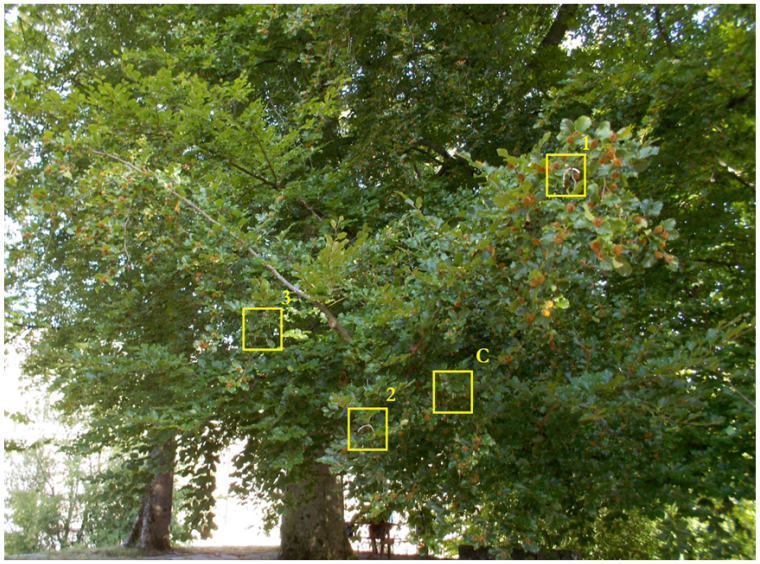

(b) Sun-exposed canopy position

Figure I: Three selected branches, including control at shaded and sun-exposed canopy positions.

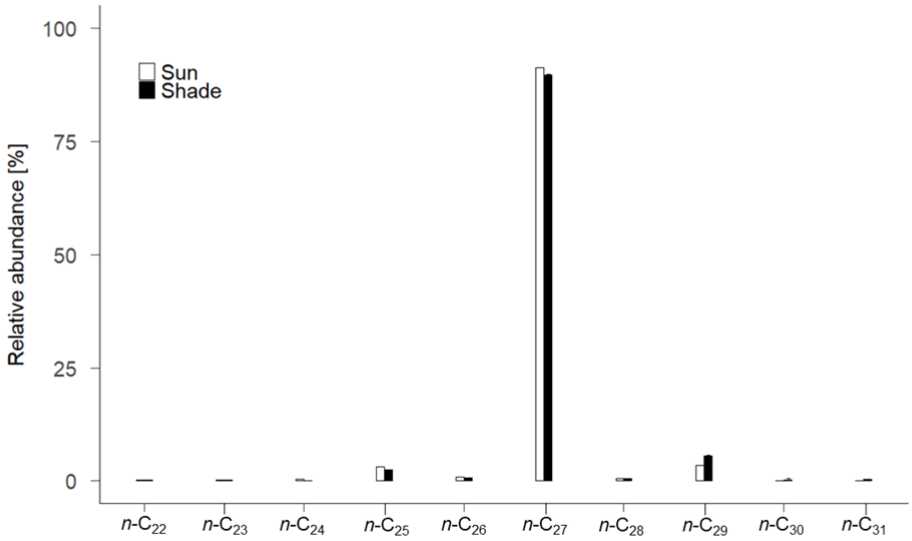

Figure II: Relative abundance of *n*-alkanes (C_{23-29}) of sun-exposed and shaded leaves. Each bar represents the average value $\pm$ sd of 20 samples of sun-exposed and shaded leaves.

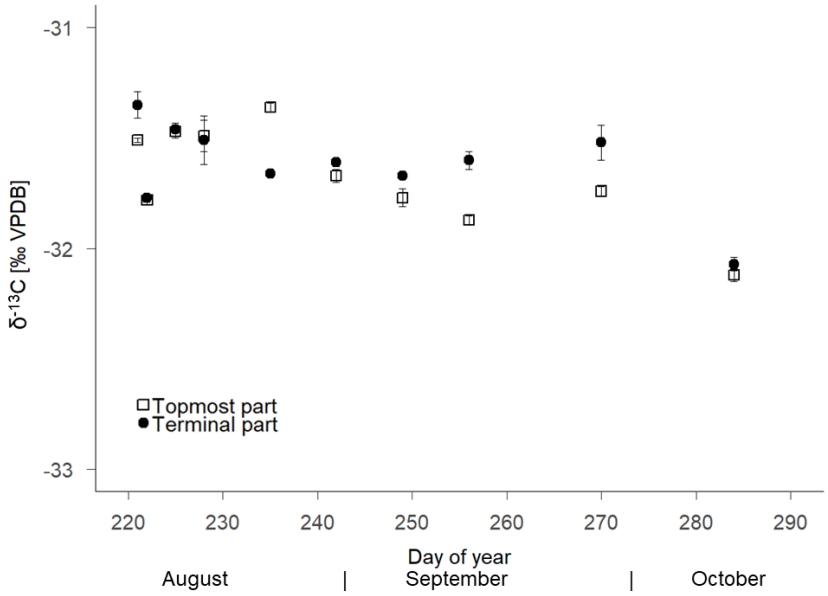

(a) Differences between δ^{13}C values of shaded leaves located on the topmost or terminal part of the branch.

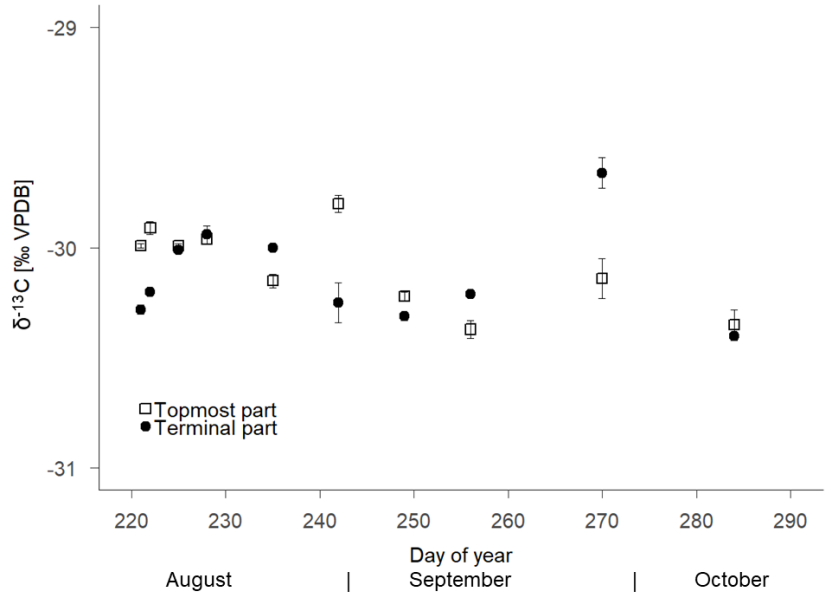

(b) Differences between δ^{13}C values of sun-exposed leaves located on the topmost or terminal part of the branch.

Figure III: Variability in the δ^{13}C values of sun-exposed and shaded leaves (n=2) located on the topmost or terminal part of the branch throughout the late growing season (Aug - Oct, 2018).The average value $\pm$ sd represents three measurement runs.

Table I: Physical leaf properties of shaded leaves throughout the late growing season (Aug - Oct, 2018). *C* = carbon, *N* = nitrogen.

DOY	Treatment	SPAD [-]	C [mg g^{-1}]	N [mg g^{-1}]	C:N	Leaf surface [cm^2]	Dry weight [mg]
221	control	34.93	43.74	1.94	22.56	120.38	227.07
221	control	36.48	43.65	2.09	20.84	77.35	165.63
221	labelling	32.65	40.42	2.03	19.92	77.87	204.25
221	labelling	34.55	43.29	2.12	20.43	66.09	130.87
221	labelling	32.35	43.18	1.90	22.67	76.72	189.93
221	labelling	32.35	42.19	1.74	24.28	82.56	216.40
221	labelling	34.50	41.81	2.00	20.92	65.37	154.29
221	labelling	34.00	44.76	2.07	21.65	62.71	151.47
222	control	32.10	44.59	2.26	19.75	87.66	160.82
222	control	30.55	43.41	2.10	20.67	60.83	139.05
222	labelling	31.55	44.28	2.09	21.18	53.68	137.31
222	labelling	35.00	45.30	2.12	21.33	85.84	307.36
222	labelling	31.90	45.39	2.32	19.53	40.70	106.21
222	labelling	33.70	42.80	2.20	19.44	51.61	162.84
222	labelling	30.70	45.52	2.06	22.14	36.48	86.28
222	labelling	33.40	44.82	2.22	20.22	53.28	152.48
225	control	30.73	42.85	1.94	22.08	35.22	75.73
225	control	32.05	43.60	2.09	20.91	47.80	98.55
225	labelling	32.70	43.11	1.97	21.87	42.92	135.56
225	labelling	34.95	45.19	2.02	22.33	59.61	226.87
225	labelling	31.80	43.57	1.98	21.99	45.80	130.13
225	labelling	33.33	44.33	2.12	20.92	55.36	162.40
225	labelling	31.35	44.03	2.03	21.67	38.38	97.96
225	labelling	33.65	42.61	2.02	21.12	65.39	174.65
228	control	29.75	44.45	1.81	24.57	52.94	119.29
228	control	31.24	44.97	2.06	21.82	40.41	120.28
228	labelling	34.40	41.42	1.87	22.13	58.79	186.87
228	labelling	34.95	44.43	2.06	21.51	54.87	181.52
228	labelling	31.30	43.80	1.99	21.97	20.08	58.15
228	labelling	33.09	44.11	2.06	21.40	49.34	155.52
228	labelling	31.50	44.40	1.97	22.56	35.37	92.52
228	labelling	31.20	43.65	1.97	22.21	36.55	87.57
235	control	30.11	45.13	2.20	20.53	23.73	58.64

DOY	Treatment	SPAD [-]	C [mg g^{-1}]	N [mg g^{-1}]	C:N	Leaf surface [cm^2]	Dry weight [mg]
235	control	32.36	45.31	2.06	21.96	74.38	118.29
235	labelling	32.69	44.70	1.97	22.73	41.11	107.28
235	labelling	30.42	44.35	1.80	24.65	28.95	142.69
235	labelling	32.88	43.46	2.02	21.49	60.24	77.96
235	labelling	30.68	43.62	2.02	21.64	34.44	181.92
235	labelling	31.71	44.05	1.91	23.02	48.43	136.38
242	control	31.50	44.95	2.13	21.06	52.65	104.82
242	control	32.39	44.23	2.05	21.62	45.63	87.96
242	labelling	33.40	43.81	1.85	23.67	59.14	248.00
242	labelling	33.93	46.30	1.88	24.61	59.29	195.97
242	labelling	32.85	43.88	2.04	21.47	39.84	117.95
242	labelling	32.08	45.20	1.90	23.77	23.71	74.02
242	labelling	31.25	44.93	1.99	22.61	38.61	97.49
242	labelling	32.67	42.68	1.95	21.88	53.77	132.90
249	control	30.70	44.40	1.98	22.40	0.00	91.17
249	control	30.52	44.53	2.06	21.57	36.45	78.03
249	labelling	32.38	46.44	2.17	21.40	51.40	135.45
249	labelling	34.05	46.08	2.03	22.68	86.52	277.03
249	labelling	32.04	45.35	2.14	21.23	35.46	109.47
249	labelling	32.42	44.83	2.12	21.12	90.78	139.63
249	labelling	31.38	44.33	1.77	25.05	46.19	84.24
249	labelling	32.48	46.01	2.13	21.61	60.58	193.19
256	control	31.29	45.37	2.10	21.62	79.41	162.78
256	control	30.36	44.40	1.84	24.10	31.46	58.25
256	labelling	32.39	45.66	1.97	23.20	99.21	267.93
256	labelling	32.22	45.72	2.19	20.87	76.83	178.12
256	labelling	30.20	46.06	2.20	20.92	57.96	112.05
256	labelling	30.20	45.32	2.27	19.92	57.01	125.46
256	labelling	30.39	45.49	2.21	20.54	49.62	82.70
256	labelling	31.93	44.36	2.08	21.34	56.14	179.68
270	control	30.08	41.03	1.76	23.37	39.27	198.81
270	control	29.93	44.55	2.04	21.88	40.51	184.66
270	labelling	30.76	45.07	1.80	24.97	47.34	148.20
270	labelling	32.76	46.26	2.07	22.36	62.35	184.14
270	labelling	32.20	44.96	2.04	22.01	63.09	174.03
270	labelling	31.16	45.48	2.09	21.81	66.36	167.72

DOY	Treatment	SPAD [-]	C [mg g^{-1}]	N [mg g^{-1}]	C:N	Leaf surface [cm^2]	Dry weight [mg]
270	labelling	30.60	45.07	2.13	21.12	53.03	118.13
270	labelling	31.60	45.58	2.18	20.91	61.58	147.24
284	control	23.90	43.50	1.87	23.20	9.80	19.36
284	control	30.40	44.29	1.86	23.87	27.17	46.95
284	labelling	30.10	45.47	1.87	24.25	11.95	39.60
284	labelling	30.00	46.34	1.95	23.80	8.33	26.68
284	labelling	28.76	45.82	1.90	24.07	27.59	74.40
284	labelling	29.03	45.10	1.98	22.74	49.02	118.60
284	labelling	30.37	44.62	1.84	24.19	78.51	198.45
284	labelling	29.37	45.63	2.12	21.50	59.52	128.95

Table II: Physical leaf properties of sun-exposed leaves throughout the late growing season (Aug - Oct, 2018). *C* = carbon, *N* = nitrogen.

DOY	Treatment	SPAD [-]	C [mg g^{-1}]	N [mg g^{-1}]	C:N	Leaf surface [cm^2]	Dry weight [mg]
221	control	36.45	42.50	1.71	24.88	40.71	124.48
221	control	30.75	44.72	1.67	26.76	70.28	201.30
221	labelling	37.55	46.31	1.59	29.07	56.19	255.72
221	labelling	33.05	45.75	1.86	24.63	35.00	237.37
221	labelling	34.80	44.45	1.73	25.71	46.34	313.75
221	labelling	34.25	45.21	1.75	25.87	45.90	173.27
221	labelling	39.30	44.50	1.91	23.33	35.23	237.57
221	labelling	37.30	44.94	2.19	20.50	37.34	251.93
222	control	32.45	44.73	1.80	24.81	34.68	147.98
222	control	36.05	43.08	1.39	30.90	47.63	235.33
222	labelling	29.20	47.17	1.52	31.11	29.28	208.14
222	labelling	30.40	47.68	1.66	28.75	39.06	268.72
222	labelling	31.30	45.21	1.62	27.90	23.65	135.10
222	labelling	34.30	45.66	1.77	25.77	16.77	118.11
222	labelling	32.60	44.40	1.98	22.40	55.14	221.87
222	labelling	32.25	46.82	1.65	28.37	22.78	126.88
225	control	34.43	43.91	1.77	24.74	50.84	216.45
225	control	37.73	45.18	1.88	24.08	43.92	231.88
225	labelling	30.80	48.43	1.77	27.34	33.81	173.15
225	labelling	36.80	46.41	1.67	27.83	15.92	182.58
225	labelling	31.80	45.66	1.62	28.21	35.82	208.31
225	labelling	35.55	46.89	1.78	26.41	46.29	305.04
225	labelling	29.48	44.73	1.80	24.82	39.16	126.16
225	labelling	33.25	47.31	1.85	25.57	48.59	255.72
228	control	33.38	45.74	1.96	23.36	59.98	231.11
228	control	34.32	45.44	1.73	26.23	47.21	192.44
228	labelling	24.06	46.38	1.25	37.16	29.95	191.28
228	labelling	32.30	45.87	1.64	27.93	33.77	237.36
228	labelling	33.80	44.37	1.79	24.72	45.08	314.41
228	labelling	36.20	45.89	1.85	24.78	31.77	269.46
228	labelling	31.40	46.17	1.75	26.40	25.78	94.25
228	labelling	31.30	46.03	1.78	25.86	39.50	164.19
235	control	33.71	45.94	1.84	24.99	45.44	176.98

DOY	Treatment	SPAD [-]	C [mg g^{-1}]	N [mg g^{-1}]	C:N	Leaf surface [cm^2]	Dry weight [mg]
235	control	35.03	45.77	1.93	23.72	28.00	127.98
235	labelling	32.60	46.45	1.63	28.44	33.20	262.71
235	labelling	33.58	46.14	1.54	29.94	36.13	296.54
235	labelling	32.46	45.53	1.84	24.78	30.86	177.29
235	labelling	36.39	47.56	2.09	22.77	37.75	310.21
235	labelling	33.25	45.07	2.14	21.02	52.61	200.58
235	labelling	31.50	46.36	1.99	23.28	32.14	165.93
242	control	33.67	44.83	1.93	23.22	41.85	152.32
242	control	34.03	45.94	1.57	29.33	56.98	224.93
242	labelling	27.98	47.46	1.23	38.46	37.03	276.11
242	labelling	29.28	48.34	1.46	33.04	31.84	150.40
242	labelling	34.59	45.77	1.59	28.81	37.66	193.97
242	labelling	34.10	46.24	1.70	27.23	38.04	237.82
242	labelling	32.21	45.23	1.95	23.22	35.46	156.07
242	labelling	28.10	45.89	1.68	27.28	20.33	98.31
249	control	32.27	45.48	1.93	23.62	66.88	127.69
249	control	34.15	45.55	1.60	28.41	41.83	154.56
249	labelling	22.04	47.21	1.10	42.76	28.39	161.42
249	labelling	30.19	47.29	1.45	32.67	36.59	161.98
249	labelling	33.65	47.81	1.95	24.47	51.72	278.87
249	labelling	35.89	48.00	1.95	24.64	32.62	238.52
249	labelling	31.60	45.54	1.93	23.58	69.07	212.79
249	labelling	30.11	47.89	1.71	28.09	34.39	129.51
256	control	32.06	45.63	1.84	24.73	23.73	216.67
256	control	30.97	45.53	1.47	30.88	74.38	266.18
256	labelling	26.96	47.00	1.34	34.97	33.71	215.15
256	labelling	25.86	48.41	1.19	40.75	38.02	167.81
256	labelling	30.40	46.57	2.04	22.85	36.19	216.21
256	labelling	34.75	46.52	1.93	24.10	50.72	282.85
256	labelling	29.93	46.24	2.13	21.74	51.01	180.61
256	labelling	32.43	47.43	2.14	22.20	48.14	201.59
270	control	33.07	44.94	1.77	25.44	91.89	161.84
270	control	37.45	45.47	1.85	24.63	92.29	245.30
270	labelling	21.90	48.05	1.14	42.28	17.32	123.66
270	labelling	31.23	48.08	1.34	35.95	42.25	370.63
270	labelling	30.54	46.44	1.80	25.86	53.34	339.81

DOY	Treatment	SPAD [-]	C [mg g^{-1}]	N [mg g^{-1}]	C:N	Leaf surface [cm^2]	Dry weight [mg]
270	labelling	32.23	47.74	1.79	26.60	27.68	187.86
270	labelling	27.63	47.53	2.08	22.90	52.64	188.84
270	labelling	28.69	48.05	1.86	25.85	54.72	297.95
284	control	31.57	45.71	1.66	27.61	30.41	108.38
284	control	24.80	44.88	1.86	24.17	40.58	175.54
284	labelling	23.10	47.43	1.09	43.66	13.26	84.89
284	labelling	10.98	48.03	0.80	60.07	33.56	274.74
284	labelling	30.66	48.39	1.83	26.48	66.30	434.39
284	labelling	29.39	48.43	1.95	24.83	9.72	198.38
284	labelling	30.52	46.78	2.08	22.54	58.80	261.78
284	labelling	27.30	49.24	1.77	27.78	64.30	313.64

Table III: Epicuticular wax content, including *n*-alkane content of shaded leaves. *EW*= epicuticular wax.

DOY	Treatment	EW content [mg]	EW content [mg g^{-2}]	EW content [μg cm^{-2}]	*n*-Alkane content [mg]	*n*-Alkane content [mg g^{-1}]	*n*-Alkane content [μg cm^{-2}]
221	control	0.89	5.93	13.80	0.32	1.99	4.96
221	labelling	1.42	9.47	18.75	0.55	2.87	7.26
222	control	0.53	3.53	5.63	0.38	1.91	4.04
222	labelling	1.55	10.33	23.65	0.41	2.06	6.26
225	control	1.15	7.67	18.59	0.26	1.89	4.20
225	labelling	1.28	8.53	24.17	0.31	1.77	5.85
228	control	1.48	9.87	22.98	0.28	2.06	4.35
228	labelling	1.25	8.33	21.24	0.39	2.07	6.63
235	control	1.60	10.67	18.62	0.41	1.98	4.77
235	labelling	1.77	11.80	21.04	0.49	1.93	5.83
242	control	1.31	8.73	19.24	0.33	1.95	4.85
242	labelling	0.99	6.60	20.11	0.32	2.15	6.50
249	control	1.14	7.60	19.66	0.28	1.93	4.83
249	labelling	1.37	9.13	18.14	0.42	1.94	5.56
256	control	1.16	7.73	21.30	0.24	1.66	4.41
256	labelling	1.04	6.93	17.40	0.32	1.88	5.35
270	control	1.90	12.67	23.26	0.40	1.74	4.90
270	labelling	1.53	10.20	18.76	0.40	2.41	4.91
284	control	1.02	6.80	27.13	0.16	1.62	4.26
284	labelling	1.25	8.33	21.87	0.29	2.41	5.07

Table IV: Epicuticular wax content, including *n*-alkane content of sun-exposed. *EW*= epicuticular wax.

DOY	Treatment	EW content [mg]	EW content [mg g^{-2}]	EW content [μg cm^{-2}]	*n*-Alkane content [mg]	*n*-Alkane content [mg g^{-1}]	*n*-Alkane content [μg cm^{-2}]
221	control	1.65	11.00	31.66	0.45	1.76	8.64
221	labelling	1.87	12.47	33.82	0.86	2.50	15.55
222	control	1.58	10.53	36.22	0.47	1.82	10.77
222	labelling	1.62	10.80	36.99	0.75	2.42	17.13
225	control	1.70	11.33	33.62	0.69	2.26	13.64

DOY	Treatment	EW content [mg]	EW content [mg g^{-2}]	EW content [μg cm^{-2}]	*n*-Alkane content [mg]	*n*-Alkane content [mg g^{-1}]	*n*-Alkane content [μg cm^{-2}]
225	labelling	1.86	12.40	39.17	0.79	2.25	16.64
228	control	1.72	11.47	32.50	0.54	2.12	10.20
228	labelling	2.56	17.07	56.61	0.87	2.33	19.24
235	control	1.94	12.93	34.54	0.61	2.04	10.86
235	labelling	2.33	15.53	42.07	0.92	2.52	16.61
242	control	1.98	13.20	35.45	0.61	1.91	10.92
242	labelling	1.72	11.47	33.82	0.83	2.21	16.32
249	control	2.30	15.33	48.84	0.50	1.84	10.62
249	labelling	1.65	11.00	33.64	0.68	1.83	13.86
256	control	2.25	15.00	42.17	0.76	2.45	14.25
256	labelling	1.78	11.87	26.75	0.96	2.29	14.43
270	control	2.06	13.73	39.64	0.65	2.03	12.51
270	labelling	1.81	12.07	37.17	0.77	1.85	15.81
284	control	1.61	10.73	42.76	0.43	1.66	11.42
284	labelling	1.83	12.20	20.12	0.74	1.89	8.14

Table V: δ^{13}C values of bulk tissue and *n*-alkanes of sun-exposed and shaded leaves. Average value $\pm$ sd represents three measurement runs.

DOY	δ^{13}C [‰VPDB] Shaded bulk tissue	δ^{13}C [‰VPDB] Shaded *n*-alkane	δ^{13}C [‰VPDB] Sun-exposed bulk tissue	δ^{13}C [‰VPDB] Sun-exposed *n*-alkane
221	-31.39 + 0.10	-34.33 + 0.04	-30.13 + 0.10	-31.32 + 0.05
222	-31.79 + 0.01	-33.98 + 0.05	-30.06 + 0.10	-31.59 + 0.03
225	-31.46 + 0.02	-34.34 + 0.07	-30.01 + 0.02	-31.21 + 0.02
228	-31.48 + 0.08	-34.20 + 0.05	-29.98 + 0.01	-31.20 + 0.05
235	-31.51 + 0.10	-34.43 + 0.14	-30.08 + 0.10	-31.57 + 0.03
242	-31.65 + 0.03	-34.41 + 0.06	-30.00 + 0.20	-32.06 + 0.12
249	-31.74 + 0.07	-34.19 + 0.08	-30.28 + 0.04	-31.23 + 0.07
256	-31.70 + 0.10	-34.24 + 0.06	-30.27 + 0.06	-31.69 + 0.13
270	-31.60 + 0.20	-34.31 + 0.10	-29.98 + 0.20	-31.24 + 0.28
284	-32.12 + 0.02	-34.55 + 0.04	-30.40 + 0.01	-31.44 + 0.09